Estimating State Price Densities via Local Polynomials

A **Master Thesis** *Presented*

by

Pierre Kervella

(164714)

to

Prof. Dr. Wolfgang Härdle

Institute for Statistics and Econometrics

in partial fulfillment of the requirements
for the degree of

Master of Statistics

Humboldt–Universität zu Berlin
Spandauer Str. 1
D–10178 *Berlin*

Berlin, March 11, 2002

Declaration of Authorship

I hereby confirm that I have authored this diploma thesis independently and without use of others than the indicated resources.

All passages, which are literally or in general matter taken out of publications or other resources, are marked as such.

Pierre Kervella

Berlin, March 11, 2002

Abstract

This master thesis aims at estimating state price densities (SPD) via a nonparametric fit of the implied volatility smile and of its derivatives. To achieve this task, we use the local polynomial estimators and apply the empirical bias–bandwidth selector (EBBS) algorithm to determine both global and local optimal bandwidths. The accuracy of the nonparametric estimates is then studied from the statistical and financial points of view. Afterwards, the resulting SPD estimates are presented as well as their bootstrap confidence bands. In a last part, we compare our semiparametric method with the implied binomial trees.

Thanks to

Wolfgang Härdle (Professor at Institute for Statistics and Econometrics of Humboldt–Universität zu Berlin), Matthias Fengler, Torsten Kleinow, Axel Werwatz (all Institue for Statistics and Econometrics of Humboldt–Universität zu Berlin), Sebastien Raspiller (INSEE), Peter Schmidt (Bankgesellschaft Berlin) for any help and advice.

Contents

1 Introduction

Since the significant advance provided by the work of Black and Scholes (1973), contingent claims are priced using the replication principle. It means that the price of a contingent claim is the cost of its perfect replication through dynamic portfolios composed of the underlying asset and bonds. The effective calculation of these prices rely on the modelling of the underlying price process as a geometric brownian motion, implying that the returns of the asset price are normally distributed. However, it is widely documented that most asset returns exhibit skewness and excess kurtosis in the unconditional distribution and heteroskedasticity in their conditional distribution. In practice, this lack of historical validity is corrected by means of the implied volatility which is the volatility parameter equalizing the theoretical and the observed price. Thus, the options market participants do not go on using statistical estimates of the underlying volatility as proxy when they price contingent claims but rather use the options extracted volatilities, also because of their forward–looking feature. Recently, this point of view has been extended to determine distributions for the underlying price implied by observed European call prices. Such an approach is meaningful since options have become liquid assets and their prices are therefore determined by the interaction between supply and demand.

There exist numerous methods to recover these distributions also called State Price Densities (SPD) empirically. They can be separated in two classes:

- methods using option prices as identifying conditions
- methods using the second derivative of the call pricing function with respect to the strike price

The first class includes methods which consist in estimating the parameters of a mixture of log–normal densities to match the observed option prices, Melick and Thomas (1997). Another popular approach in this class is the implied binomial trees method, see Rubinstein (1994), Derman and Kani (1994) and Härdle, Kleinow and Stahl (2002). Another technique is based on learning networks suggested by Hutchinson, Lo and Poggio (1994), a nonparametric approach using artificial neural networks, radial basis functions, and projection pursuits.

The second class of methods is based on the seminal work of Breeden and Litzenberger (1978), which proves that the state price density is equal to the second derivative of the call pricing function with respect to the strike K. Aït–Sahalia and Lo (1998)

use this result as basis to estimate semiparametrically the SPD. Their work as well as the paper of Rookley (1997) paved the way to this study. Actually, this paper is based on Rookley's semiparametric technique which uses a nonparametric regression of the implied volatility function and of its derivatives.

Once these distributions also called state price densities (SPD) are estimated, they may serve for pricing new, complex or illiquid derivative securities. Indeed, the price of a security at time t (P_t) with a single liquidation date T and payoff $Z(S_T)$ is:

$$P_t = e^{-r_{t,\tau}\tau} \int_{-\infty}^{\infty} Z(S_T) f_t^*(S_T) dS_T \tag{1}$$

where S_T is the state variable, $r_{t,\tau}$ is the risk–free rate at time t with time to maturity τ, and $f_t^*(S_T)$ is the SPD at time t for date T payoffs. Moreover, they provide the market participants with a rich source of information for assessing the market sentiment.

This master thesis begins in section 2 with the explanation of the Breeden and Litzenberger result along with its first application, the Black and Scholes SPD. In the third part, different non– and semiparametric models and several frameworks are exposed. In section 4, the nonparametric estimators necessary to get our semiparametric SPD are expounded with a discussion on the Empirical Bias–Banwidth Selector algorithm (EBBS). Then, in section 5, the data are presented and in the next section a comparison between the different nonparametric estimates is conducted. In section 7, we present the obtained SPD estimates and develop a method to compute confidence bands. The last section compares our SPD estimates with those obtained by the implied binomial trees.

2 Extracting the SPD using European options

2.1 The Breeden & Litzenberger result

Breeden and Litzenberger (1978) show that one can replicate Arrow–Debreu prices using the concept of *butterfly spread* on European call options. On the one hand, an Arrow–Debreu security is a theoretical contingent claim paying one currency unit if a certain state of the economy happens at a given future date (here, the states of the economy are restricted to the possible values of one asset). On the other hand, the butterfly spread exists in practice as linear combination of call options. Indeed, it entails selling two call options at exercise price K, buying one call option at $K^- = K - \Delta K$ and another at $K^+ = K + \Delta K$, where ΔK is the stepsize between the adjacent call strikes. These four options constitute a butterfly spread centered on K. If the terminal underlying asset value S_T is equal to K then the payoff $Z(\cdot)$ of $\frac{1}{\Delta K}$ of such butterfly spreads is defined as:

$$Z(S_T, K; \Delta K) = P(S_{T-\tau}, \tau, K; \Delta K)|_{\tau=0} = \left.\frac{u_1 - u_2}{\Delta K}\right|_{S_T=K,\tau=0} = 1 \tag{2}$$

where

$$u_1 = C(S_{T-\tau}, \tau, K + \Delta K) - C(S_{T-\tau}, \tau, K),$$
$$u_2 = C(S_{T-\tau}, \tau, K) - C(S_{T-\tau}, \tau, K - \Delta K).$$

$C(S, \tau, K)$ denotes the price of a European call with an actual underlying price S, a time to maturity τ and a strike price K. Here, $P(S_{T-\tau}, \tau, K; \Delta K)$ is the corresponding price of this security ($\frac{1}{\Delta K} * butterfly\ spread(K; \Delta K)$) at time $T - \tau$.

As ΔK tends to zero, this security becomes an Arrow–Debreu security paying 1 if $S_T = K$ and zero in other states. As it is assumed that S_T has a continuous distribution function on $\mathbb{R}^+$, the probability of any given level of S_T is zero and thus, in this case, the price of an Arrow–Debreu security is zero. However, dividing one more time by ΔK, one obtains the price of ($\frac{1}{(\Delta K)^2} * butterfly\ spread(K; \Delta K)$) and as ΔK tends to 0 this price tends to $f^*(S_T)e^{-r_{t,\tau}}$ for $S_T = K$. Indeed,

$$\lim_{\Delta K \to 0} \left(\frac{P(S_t, \tau, K; \Delta K)}{\Delta K} \right) \Bigg|_{K=S_T} = f^*(S_T)e^{-r_{t,\tau}}. \tag{3}$$

This can be proved by setting the payoff Z_1 of this new security

$$Z_1(S_T) = \left(\frac{1}{(\Delta K)^2} (\Delta K - |S_T - K|) \mathbf{1}_{S_T \in [K - \Delta K, K + \Delta K]} \right) \tag{4}$$

in (1) and letting ΔK tend to 0. One should also notice that:

$$\forall(\Delta K) : \int_{K-\Delta K}^{K+\Delta K} (\Delta K - |S_T - K|) dS_T = (\Delta K)^2.$$

If one can construct these financial instruments on a continuum of states (strike prices) then at infinitely small ΔK a complete state pricing function can be defined. Moreover, as ΔK tends to zero, this price will tend to the second derivative of the call pricing function with respect to (w.r.t.) the strike price evaluated at K:

$$\begin{aligned} \lim_{\Delta K \to 0} \left(\frac{P(S_t, \tau, K; \Delta K)}{\Delta K} \right) &= \lim_{\Delta K \to 0} \frac{u_1 - u_2}{(\Delta K)^2} \\ &= \frac{\partial^2 C_t(\cdot)}{\partial K^2}. \end{aligned} \tag{5}$$

Equating (3) and (5) across all states yields:

$$\left. \frac{\partial^2 C_t(\cdot)}{\partial K^2} \right|_{K=S_T} = e^{-r_{t,\tau}\tau} f_t^*(S_T)$$

where $r_{t,\tau}$ denotes the risk–free interest rate at time t with time to maturity τ and $f_t^*(\cdot)$ denotes the risk–neutral PDF or the SPD in t. Therefore, the SPD is defined as:

$$f_t^*(S_T) = e^{r_{t,\tau}\tau} \left. \frac{\partial^2 C_t(\cdot)}{\partial K^2} \right|_{K=S_T}. \tag{6}$$

This method constitutes a no–arbitrage approach to recover the SPD. No assumption on the underlying asset dynamics are required. Preferences are not restricted. The only requirements for this method are that markets are perfect (i.e. no sales restrictions, transactions costs or taxes and that agents are able to borrow at the risk–free interest rate) and that $C(\cdot)$ is twice differentiable. The same result can be obtained by differentiating (1) twice w.r.t. K after setting for Z the call payoff function $Z(S_T) = (S_T - K)^+$. Remark that f^* is called State–Price Density since $f_t^*(K)$ represents the price that the market is ready to pay at time t to get one unit of currency if the state $S_T \in [K, K + dK]$ occurs at time T.

Since this methodology is based on European calls, it may not be applied to all options on the market. Typically, this method is advocated for index options whose liquidity is sufficient. Since in–the–money options are usually not liquid, in–the–money call prices are determined using out-of-the-money puts and the Put–Call parity relation. Moreover, this result also assumes a continuum of strike prices on $\mathbb{R}^+$ which can not be found on any stock exchange. Indeed, the strike prices are always discretely spaced on a finite range around the actual underlying price. Hence, most of the procedures relying on this result (including the one presented here) try to handle this

problem by interpolating the call pricing function inside the range and extrapolating it outside. In Section 3, semiparametric models using nonparametric regression of the implied volatility will be introduced to provide this interpolation task. However, a first application of this result is to determine the SPD implied by the Black–Scholes model.

2.2 Black–Scholes SPD

The Black–Scholes call option pricing formula is due to Black and Scholes (1973) and Merton (1973). In this model there are no assumptions regarding preferences, rather it relies on no–arbitrage conditions and assumes that the evolution of the underlying asset price S_t follows a geometric Brownian motion defined through

$$\frac{dS_t}{S_t} = \mu dt + \sigma dW_t. \tag{7}$$

Here μ denotes the drift and σ the volatility assumed to be constant.
The analytical formula for the price in t of a call option with a terminal date $T = t+\tau$, a strike price K, an underlying price S_t, a risk–free rate $r_{t,\tau}$, a continuous dividend yield $\delta_{t,\tau}$, and a volatility σ, is:

$$\begin{aligned} C_{BS}(S_t, K, \tau, r_{t,\tau}, \delta_{t,\tau}; \sigma) &= e^{-r_{t,\tau}} \int_0^\infty \max(S_T - K, 0) f^*_{BS,t}(S_T) dS_T \\ &= S_t e^{-\delta_{t,\tau}} \Phi(d_1) - K e^{-r_{t,\tau}\tau} \Phi(d_2) \end{aligned}$$

where $\Phi(\cdot)$ is the standard normal cumulative distribution function and

$$\begin{aligned} d_1 &= \frac{\log(S_t/K) + (r_{t,\tau} - \delta_{t,\tau} + \frac{1}{2}\sigma^2)\tau}{\sigma\sqrt{\tau}}, \\ d_2 &= d_1 - \sigma\sqrt{\tau}. \end{aligned}$$

As a consequence of the assumptions on the underlying asset price process the Black–Scholes SPD is a log–normal density with mean $(r_{t,\tau} - \delta_{t,\tau} - \frac{1}{2}\sigma^2)\tau$ and variance $\sigma^2\tau$ for $\log(S_T/S_t)$:

$$\begin{aligned} f^*_{BS,t}(S_T) &= e^{r_{t,\tau}\tau} \frac{\partial^2 C_t}{\partial K^2}\bigg|_{K=S_T} \\ &= \frac{1}{S_T\sqrt{2\pi\sigma^2\tau}} \exp\left[- \frac{[\log(S_T/S_t) - (r_{t,\tau} - \delta_{t,\tau} - \frac{1}{2}\sigma^2)\tau]^2}{2\sigma^2\tau} \right]. \end{aligned}$$

The risk measures Delta (Δ) and Gamma (Γ) are defined as:

$$\Delta_{BS} \stackrel{\text{def}}{=} \frac{\partial C_{BS}}{\partial S_t} = \Phi(d_1)$$
$$\Gamma_{BS} \stackrel{\text{def}}{=} \frac{\partial^2 C_{BS}}{\partial S_t^2} = \frac{\Phi(d_1)}{S_t\sigma\sqrt{\tau}}$$

The Black–Scholes SPD can be calculated in XploRe using the following quantlet:

```
bsspd = spdbs(K,s,r,div,sigma,tau)
```

computes the Black–Scholes SPD.

The arguments are the strike prices (`K`), underlying price (`s`), risk–free interest rate (`r`), dividend yields (`div`), implied volatility of the option (`sigma`), and the time to maturity (`tau`). The output consist of the Black–Scholes SPD (`bsspd.fbs`), Δ (`bsspd.delta`), and the Γ (`bsspd.gamma`) of the call options. Please note that `spdbs` can be applied to put options after calculating their corresponding call prices using the Put–Call parity.

However, it is widely known that the Black–Scholes call option formula is not valid empirically. One of the problems is that the implied volatility σ in the Black–Scholes model is supposed to be constant over the maturity direction and strike prices (or equivalently moneyness). Visual inspection of most option data will show that a volatility smile (or skew) is present in the moneyness direction and that implied volatilities also change with the maturity of the corresponding options (see Härdle et al. (2002) for more details). Those features of the implied volatility surface is a consequence of the 1987' crash which resulted in an increase of the demand for protective puts, mainly by the fund managers.

Since the Black–Scholes model contains empirical irregularities, its SPD will not be consistent with the data. Consequently, some other techniques for estimating the SPD without any assumptions on the underlying diffusion process have been developed in the last years.

3 Semiparametric models

3.1 Nonparametric and semiparametric models for the call pricing function

The use of nonparametric regression to recover the SPD was first investigated by Aït–Sahalia and Lo (1998). They propose to use the Nadaraya–Watson estimator to estimate the historical call prices $C_t(\cdot)$ as a function of the following state variables $(S_t, K, \tau, r_{t,\tau}, \delta_{t,\tau})^\top$. Kernel regressions are advocated because there is no need to specify a functional form and the only required assumption is that the function is smooth and differentiable, Härdle (1990). Nevertheless, when the regressor dimension is 5, the estimator is inaccurate in practice owing to the so called "Curse of dimensionality". This problem refers to the fact that a local neighborhood in high dimension is not always local since a neighborhood with a fixed percentage of sample points can be very big and then far from being "local". Hence, there is a need to reduce the dimension or equivalently the number of regressors. One method is to appeal to no–arbitrage arguments and collapse S_t, $r_{t,\tau}$ and $\delta_{t,\tau}$ into the forward price $F_t = S_t e^{(r_{t,\tau}-\delta_{t,\tau})\tau}$ in order to express the call pricing function as:

$$C(S_t, K, \tau, r_{t,\tau}, \delta_{t,\tau}) = C(F_{t,\tau}, K, \tau, r_{t,\tau}). \tag{8}$$

An alternative specification assumes that the call option function is homogeneous of degree one in S_t and K (as in the Black–Scholes formula) so that:

$$C(S_t, K, \tau, r_{t,\tau}, \delta_{t,\tau}) = KC(S_t/K, \tau, r_{t,\tau}, \delta_{t,\tau}). \tag{9}$$

Combining the assumptions of (8) and (9) the call pricing function can be further reduced to a function of three variables $(\frac{K}{F_{t,\tau}}, \tau, r_{t,\tau})$. The first variable $\frac{K}{F_{t,\tau}}$ is generally called moneyness. Indeed, this term is the result of the language convention which calls the options whose intrinsic value $(S_t - K)^+$ is positive "in the money". The options with a strike nearly equal to the underlying spot price are said to be "at the money" and in the last case, they are "out of the money". Nevertheless, in the literature, this term refers to different ratios involving the underlying price (spot or forward) and the strike price of the option. Therefore, we interchangeably use the term moneyness for $m = \frac{K}{F_{t,\tau}}$ and $m = \frac{S_T}{K}$.

Another approach is to use a semiparametric model based on the Black–Scholes formula. Here, the call pricing function is parametric based on the Black–Scholes model

while the implied volatility σ is modelled as a nonparametric function. One needs to estimate the implied volatility as the following nonparametric function, $\sigma(F_{t,\tau}, K, \tau)$, consequently:

$$C(S_t, K, \tau, r_{t,\tau}, \delta_{t,\tau}) = C_{BS}(F_{t,\tau}, K, \tau, r_{t,\tau}; \sigma(F_{t,\tau}, K, \tau)).$$

It is widely known that empirically the implied volatility function mostly depends on two parameters: the time to maturity τ and the moneyness $M = X/F_{t,\tau}$. Almost equivalently, one can set $M = \tilde{S}_t/X$ where $\tilde{S}_t = S_t - D$ and D is the present value of the dividends to be paid before the expiration. Actually, in the case of a dividend yield δ_t, we have $D = S_t(1-e^{-\delta_t})$. If the dividends are discrete, then $D = \sum_{t_i \leq t+\tau} D_{t_i} e^{-r_{t,\tau_i}}$ where t_i is the dividend payment date of the i^{th} dividend and τ_i is its maturity. Therefore, the dimension of the implied volatility function can be reduced to $\sigma(X/F_{t,\tau}, \tau)$. In this case the call option function is:

$$C(S_t, X, \tau, r_{t,\tau}, \delta_{t,\tau}) = C_{BS}(F_{t,\tau}, X, \tau, r_{t,\tau}; \sigma(X/F_{t,\tau}, \tau)).$$

To estimate $\hat{C}_t(\cdot)$ and $\hat{f}_t^* = e^{r_{t,\tau}\tau}\left[\frac{\partial^2 \hat{C}_t(\cdot)}{\partial X^2}\right]$, one has to choose a nonparametric method (Nadaraya–Watson, local polynomials,...), a Kernel function and some smoothing parameters. In the case of a Nadaraya–Watson estimator, the order of the Kernel function is a key issue for estimating the derivatives, Aït–Sahalia and Lo (1998). However, the method presented in this survey is based on a different semiparametric model presented in the following section.

3.2 A semiparametric model for the SPD

The previous section proposed a semiparametric estimator of the call pricing function and the corresponding approach to recover the SPD. In this section the dimension is reduced further using mathematical derivations provided by Rookley Rookley (1997).

Fixing the maturity allows us to eliminate τ from the specification of the implied volatility function. In the following part, for convenience, the definition of the moneyness is $M = \tilde{S}_t/K$ and we denote by σ the implied volatility. The notation $\frac{\partial f(x_1,\ldots,x_n)}{\partial x_i}$ denotes the partial derivative of f w.r.t. x_i and $\frac{\mathrm{d}f(x)}{\mathrm{d}x}$ the total derivative of f with respect to x. Moreover, the following rescaled call option function is used:

$$\begin{aligned} c_{it} &= \frac{C_{it}}{\tilde{S}_t}, \\ M_{it} &= \frac{\tilde{S}_t}{K_i}. \end{aligned}$$

where C_{it} is the price of the i^{th} option at time t.

The rescaled call option function can be expressed as:

$$\begin{aligned} c_{it} &= c(M_{it}; \sigma(M_{it})) = \Phi(d_1) - \frac{e^{-r\tau}\Phi(d_2)}{M_{it}}, \\ d_1 &= \frac{\log(M_{it}) + \left\{r_t + \frac{1}{2}\sigma(M_{it})^2\right\}\tau}{\sigma(M_{it})\sqrt{\tau}}, \\ d_2 &= d_1 - \sigma(M_{it})\sqrt{\tau}. \end{aligned}$$

The standard risk measures are then the following partial derivatives (for notational convenience subscripts are dropped):

$$\Delta = \frac{\partial C}{\partial S} = \frac{\partial C}{\partial \tilde{S}} = c(M, \sigma(M)) + \tilde{S}\frac{\partial c}{\partial \tilde{S}},$$

$$\Gamma = \frac{\partial \Delta}{\partial S} = \frac{\partial^2 C}{\partial S^2} = \frac{\partial^2 C}{\partial \tilde{S}^2} = 2\frac{\partial c}{\partial \tilde{S}} + \tilde{S}\frac{\partial^2 c}{\partial \tilde{S}^2}.$$

where

$$\begin{aligned} \frac{\partial c}{\partial \tilde{S}} &= \frac{\mathrm{d}c}{\mathrm{d}M}\frac{\partial M}{\partial \tilde{S}} = \frac{\mathrm{d}c}{\mathrm{d}M}\frac{1}{K}, \\ \frac{\partial^2 c}{\partial \tilde{S}^2} &= \frac{\mathrm{d}^2 c}{\mathrm{d}M^2}\left(\frac{1}{K}\right)^2. \end{aligned}$$

The SPD is then the second derivative of the call option function with respect to the strike price:

$$f^*(\cdot) = e^{r\tau}\frac{\partial^2 C}{\partial K^2} = e^{r\tau}\tilde{S}\frac{\partial^2 c}{\partial K^2}. \tag{14}$$

The conversion is needed because $c(\cdot)$ is being estimated not $C(\cdot)$. The analytical expression of (14) depends on:

$$\frac{\partial^2 c}{\partial K^2} = \frac{\mathrm{d}^2 c}{\mathrm{d}M^2}\left(\frac{M}{K}\right)^2 + 2\frac{\mathrm{d}c}{\mathrm{d}M}\frac{M}{K^2}$$

The functional form of $\frac{\mathrm{d}c}{\mathrm{d}M}$ is:

$$\frac{\mathrm{d}c}{\mathrm{d}M} = \Phi'(d_1)\frac{\mathrm{d}d_1}{\mathrm{d}M} - e^{-r\tau}\frac{\Phi'(d_2)}{M}\frac{\mathrm{d}d_2}{\mathrm{d}M} + e^{-r\tau}\frac{\Phi(d_2)}{M^2}, \tag{15}$$

while $\frac{\mathrm{d}^2 c}{\mathrm{d}M^2}$ is:

$$\begin{aligned} \frac{\mathrm{d}^2 c}{\mathrm{d}M^2} &= \Phi'(d_1)\left[\frac{\mathrm{d}^2 d_1}{\mathrm{d}M^2} - d_1\left(\frac{\mathrm{d}d_1}{\mathrm{d}M}\right)^2\right] \\ &- \frac{e^{-r\tau}\Phi'(d_2)}{M}\left[\frac{\mathrm{d}^2 d_2}{\mathrm{d}M^2} - \frac{2}{M}\frac{\mathrm{d}d_2}{\mathrm{d}M} - d_2\left(\frac{\mathrm{d}d_2}{\mathrm{d}M}\right)^2\right] \\ &- \frac{2e^{-r\tau}\Phi(d_2)}{M^3} \end{aligned} \tag{16}$$

The quantities in (15) and (16) are a function of the following first derivatives:

$$\begin{aligned}
\frac{\mathrm{d}d_1}{\mathrm{d}M} &= \frac{\partial d_1}{\partial M} + \frac{\partial d_1}{\partial \sigma}\frac{\partial \sigma}{\partial M}, \\
\frac{\mathrm{d}d_2}{\mathrm{d}M} &= \frac{\partial d_2}{\partial M} + \frac{\partial d_2}{\partial \sigma}\frac{\partial \sigma}{\partial M}, \\
\frac{\partial d_1}{\partial M} &= \frac{\partial d_2}{\partial M} = \frac{1}{M\sigma\sqrt{\tau}}, \\
\frac{\partial d_1}{\partial \sigma} &= -\frac{\log(M)+r\tau}{\sigma^2\sqrt{\tau}} + \frac{\sqrt{\tau}}{2}, \\
\frac{\partial d_2}{\partial \sigma} &= -\frac{\log(M)+r\tau}{\sigma^2\sqrt{\tau}} - \frac{\sqrt{\tau}}{2}.
\end{aligned}$$

The quantities in (15) and (16) also rely on the following second derivative functions:

$$\begin{aligned}
\frac{\mathrm{d}^2 d_1}{\mathrm{d}M^2} &= -\frac{1}{M\sigma\sqrt{\tau}}\left[\frac{1}{M} + \frac{V'}{\sigma}\right] + V''\left(\frac{\sqrt{\tau}}{2} - \frac{\log(M)+r\tau}{\sigma^2\sqrt{\tau}}\right) \\
&+ V'\left[2V'\frac{\log(M)+r\tau}{\sigma^3\sqrt{\tau}} - \frac{1}{M\sigma^2\sqrt{\tau}}\right], \qquad (17)
\end{aligned}$$

$$\begin{aligned}
\frac{\mathrm{d}^2 d_2}{\mathrm{d}M^2} &= -\frac{1}{M\sigma\sqrt{\tau}}\left[\frac{1}{M} + \frac{V'}{\sigma}\right] - V''\left(\frac{\sqrt{\tau}}{2} + \frac{\log(M)+r\tau}{\sigma^2\sqrt{\tau}}\right) \\
&+ V'\left[2V'\frac{\log(M)+r\tau}{\sigma^3\sqrt{\tau}} - \frac{1}{M\sigma^2\sqrt{\tau}}\right]. \qquad (18)
\end{aligned}$$

The following quantities are required to complete the computation of (17)-(18):

$$\begin{aligned}
V &= \sigma(M), \\
V' &= \frac{\partial \sigma(M)}{\partial M}, \\
V'' &= \frac{\partial^2 \sigma(M)}{\partial M^2}. \qquad (19)
\end{aligned}$$

The SPD estimation based on this last semiparametric model can be calculated with the following quantlet:

```
{fstar,delta,gamma} = spdbl(m,sigma,sigma1,sigma2,s,r,tau)
```

computes the SPD using Breeden and Litzenberger result and the derivations presented here.

The arguments for this quantlet are the moneyness `m`, V (`sigma`), V' (`sigma1`), V'' (`sigma2`), the underlying price (`s`) corrected for future dividends, the risk–free interest rate (`r`), and the time to maturity (`tau`). The output consist of the local polynomial SPD (`fstar`), Δ (`delta`), and the Γ (`gamma`) of the call–options.

3.3 Possible frameworks using these semiparametric models

Even if the two semiparametric models presented in this section are based on the same parametric model (i.e. Black–Scholes), they do not rely on the same nonparametric estimates. The first one only needs the fit of the implied volatility smile (or surface) and the second one uses also its two first derivatives with respect to the strike price K.

The SPD estimates also depend on the nonparametric method. Indeed, using Nadaraya–Watson estimators or local polynomials may yield different results. Aït–Sahalia and Duarte (2001) provide an example where local polynomials of different orders returns different results in the case of the first semiparametric model.

Furthermore, another key issue is the type of data which serve as basis for the study. Indeed, one may use settlement prices, intra–day prices or intra–day bid–ask spreads. Moreover, depending on the purpose of the study, the number of trading days used to estimate one SPD may also vary. In Aït–Sahalia and Lo (1998), many days serve as basis to recover one SPD. Otherwise Rookley (1997) uses one day of tick data for one cross section (series) of options.

Here, the framework is slightly different, as only one day of settlement data is used and the purpose is to estimate the SPD for all τ, even if τ does not correspond to the maturity of a series of option. This task is achieved by the nonparametric regression of the whole implied volatility surface and of its derivatives. This framework allows to survey the dynamics of these SPDs or their stability, as one can compare SPDs with the same theoretical maturity for different dates. Moreover, by choosing to get the SPD on a moneyness metric ($S_T/F_{t,T-t}$), one would also avoid the effect of the underlying price movement on the mean of the distribution.

Before discussing the results of the SPD estimation, the nonparametric approach chosen for this study is presented.

4 Local polynomial estimation

Since derivatives of the implied volatility curve must be fitted, local polynomials are adviseable. We introduce them in the multivariate case and then discuss the choice of the smoothing parameter.

4.1 Framework and theory

We assume an heteroscedastic model:

$$Y_i = m(X_i) + \sigma(X_i)\varepsilon_i, \quad i = 1, \ldots, n$$

where $X_i = (X_{i1}, \ldots, X_{id})$ is the d–dimensional vector of independent variables and Y_i is the response. Here, $m(\cdot)$ and $\sigma(\cdot)$ are smooth functions specifying the conditional mean and standard deviation of Y_i given X_i and ε_i has mean 0 and variance 1.

Furthermore, the ε_i's are mutually independent and the X_i's can be fixed or random. However, the latter case will not be considered as in the present study the regressors are deterministic. The goal of this method is to estimate $m(\cdot)$ and/or its derivatives.

Suppose that the $(p+1)^{th}$ derivatives of $m(\cdot)$ at the point x_0 exist. It is then possible to approximate the unknown function $m(\cdot)$ by a local polynomial of order p. Indeed, this approximation is based on a Taylor expansion which gives for x in a neighborhood of x_0,

$$\begin{aligned} m(x) \approx m(x_0) &+ \sum_{i=1}^{d} \left(\left.\frac{\partial m}{\partial x_i}\right|_{x_0} (x_i - x_{0i}) \right) \\ &+ \frac{1}{2!} \sum_{i_1=1}^{d} \sum_{i_2=1}^{d} \left(\left.\frac{\partial^2 m}{\partial x_{i_1} \partial x_{i_2}}\right|_{x_0} (x_{i_1} - x_{0i_1})(x_{i_2} - x_{0i_2}) \right) \\ &+ \cdots + \frac{1}{p!} \sum_{i_1=1}^{d} \cdots \sum_{i_p=1}^{d} \left(\left.\frac{\partial^p m}{\partial x_{i_1} \cdots \partial x_{i_p}}\right|_{x_0} \prod_{l=1}^{p} (x_{i_l} - x_{0i_l}) \right) \end{aligned}$$

or in different notation

$$m(x) \approx \sum_{S=0}^{p} \sum_{s_1+\cdots+s_d=S} \left(\prod_{j=1}^{d} (s_j!) \right)^{-1} \left. \frac{\partial^S m}{\partial x_1^{s_1} \cdots \partial x_d^{s_d}} \right|_{x_0} \prod_{j=1}^{d} (x_j - x_{0j})^{s_j}. \tag{20}$$

Observe that $\left(\prod_{j=1}^{d} (s_j!) \right)^{-1} \left. \frac{\partial^S m}{\partial x_1^{s_1} \cdots \partial x_d^{s_d}} \right|_{x_0}$ can be seen as polynomial coefficients.

The local polynomial (provided by the Taylor expansion) can then be fitted by weighted least squares regression problem whose solution $\hat{\beta}(x_0)$ is defined through:

$$\min_{\beta} \sum_{i=1}^{n} \left\{ Y_i - P_p(x_0, X, \beta) \right\}^2 K_h(X_i - x_0) \tag{21}$$

where n is the number of observations, h is a d–dimensional vector of bandwidths controlling the neighborhood in each direction and $K_h = K(\cdot/h)/h^d$ is the resulting kernel function weighting all observation points. This Kernel function may be a product of univariate Kernel functions or a multivariate Kernel. Moreover, P_p is defined through:

$$P_p(x_0, X, \beta) = \sum_{S=0}^{p} \sum_{s_1+\cdots+s_d=S} \beta_{s_1,\ldots,s_d} \prod_{j=1}^{d} (X_j - x_{0j})^{s_j} \tag{22}$$

where $\beta = \{\beta_{s_1,\ldots,s_d} : \ s_1 + \cdots + s_d = S \quad \text{and} \quad S = 0, \ldots, p\}$ is the vector of polynomial coefficients. Comparing (20) and (22), one can remark that $\forall s = (s_1, \ldots, s_d)$ such that $\sum_{i=1}^{d} s_i = S \leq p : \ m^{(s)}(x_0) = \left(\frac{\partial^S m}{\partial x_1^{s_1} \cdots \partial x_d^{s_d}} \Big|_{x_0} \right)$ can be estimated by

$$\hat{m}^{(s)}(x_0) = \left(\prod_{j=1}^{d} (s_j!) \right) \hat{\beta}_{s_1,\ldots,s_d}.$$

For convenience use the following matrix definitions:

$$\mathcal{X} = \begin{pmatrix} 1 & X_{11} - x_{01} & \cdots & X_{1d} - x_{0d} & \cdots & (X_{1d} - x_{0d})^p & \cdots & \prod_{j=1}^{d} (X_{1j} - x_{0j}) \\ \vdots & \vdots & & \vdots & & \vdots & & \vdots \\ 1 & X_{n1} - x_{01} & \cdots & X_{nd} - x_{0d} & \cdots & (X_{nd} - x_{0d})^p & \cdots & \prod_{j=1}^{d} (X_{nj} - x_{0j}) \end{pmatrix}, \tag{23}$$

$$Y = \begin{pmatrix} Y_1 \\ \vdots \\ Y_n \end{pmatrix}, \quad W = diag\{K_h(X_i - x_0)\} \quad \text{and} \quad \hat{\beta} = \begin{pmatrix} \hat{\beta}_{0,\ldots,0} \\ \vdots \\ \hat{\beta}_{1,\ldots,1} \end{pmatrix}.$$

Here $\mathcal{X}$ is a $n \times \left(\sum_{S=0}^{p} C_{d+S-1}^{S}\right)$ matrix, W is a $n \times n$ matrix and β is a vector whose dimension is $\left(\sum_{S=0}^{p} C_{d+S-1}^{S}\right)$ (C denotes the combinatorial coefficient). Hence, the weighted least squares problem (21) may be written in the following way:

$$\min_{\beta} \ (Y - \mathcal{X}\beta)^\top W (Y - \mathcal{X}\beta)$$

whose solution is provided by the weighted least squares theory and is given by

$$\hat{\beta}(x_0) = (\mathcal{X}^\top W \mathcal{X})^{-1} \mathcal{X}^\top W Y.$$

At this stage it is easy to observe that local polynomials provide a powerful tool to estimate nonparametrically an unknown function and its derivatives. Moreover, local polynomial procedure provides estimates of the function and of all its derivatives (smaller than the degree p of the polynomial) in one step.

The conditional bias and variance of the estimator $\hat{\beta}$ can be derived directly from (24):

$$\begin{aligned} \mathrm{E}(\hat{\beta}|(X_i)_{i=1,\ldots,n}) &= (\mathcal{X}^\top W \mathcal{X})^{-1} \mathcal{X}^\top W m \\ &= \beta + (\mathcal{X}^\top W \mathcal{X})^{-1} \mathcal{X}^\top W r \\ \mathrm{Var}(\hat{\beta}|(X_i)_{i=1,\ldots,n}) &= (\mathcal{X}^\top W \mathcal{X})^{-1} (\mathcal{X}^\top W \Sigma W \mathcal{X}) (\mathcal{X}^\top W \mathcal{X})^{-1}, \end{aligned} \tag{24}$$

where $m = \{m(X_1), \ldots, m(X_n)\}^\top$ contains the value of the true function at the observation points, $r = m - \mathcal{X}\beta$ is the vector of residuals of the local polynomial approximation and $\Sigma = diag\{\sigma^2(X_i)\}$. However, it is not possible to calculate these values directly since m, r and Σ are unknown.

One of the issues regarding this estimation method is the dependence on the bandwidth h which governs how much weight the Kernel function should place on an observed point for the estimation at a target point. Moreover, as the call options are not always symmetrically and equally distributed around the at–the–money point, the choice of the bandwidth is a key issue, especially for estimation at the border of the implied volatility smile or surface. Typically, the bandwidth can be chosen global or locally dependent on x_0. In both cases, there are methods providing "optimal" bandwidths which respectively rely on plug–in rules and data–based selectors. An algorithm called Empirical–Bias Bandwidth Selector (EBBS) for finding local bandwidths is suggested by Ruppert (1997). This algorithm will be explained in the following part and tested on implied volatility data in Section 6.

Other concerns in local polynomial fitting are the choices of the the local polynomial order p and the Kernel function to be used. Indeed, there is an implied bound for p since it is only possible to estimate a derivative of order S if $p \geq S$. Thus, if one is only interested in the function itself, one may used polynomials of order 0, also called Nadaraya–Watson estimators. Nevertheless Fan and Gijbels (1996) prove that the polynomial order is to be taken such that $p - S = 2q + 1$ to limit the variability of the estimates and they recommend to set $q = 0$ since the model complexity has to be driven mainly by the bandwidth. This comment implies that Nadaraya–Watson estimators are not optimal even for estimating the function itself. For the Kernel, they advise the Epanechnikov one and restrict the choice to nonnegative Kernel. However, the choice of the Kernel function is less crucial than the bandwidth one.

The quantlet `lplocband` developed for this study provides an easy way to estimate m or one of its derivative in XploRe via local polynomials:

`{f,variance} = lplocband(x, y, h, xgrid, OrderDer, p, RidgeCoef {, Kernel})`

fits the unknown function m or one of its derivative via local polynomials.

The arguments are `x` a matrix of regressors, `y` the dependent variable, `h` the bandwidth (local or global), `xgrid` the grid of target points, `OrderDer` the order of the derivative to be estimated, `p` the order of the polynomial, `RidgeCoef` the parameter of the ridge regression if desired and `Kernel` is a string containing the Kernel function to be used. The output consists of `f` the estimated derivative at all target points in `xgrid` and of `variance` an estimate of the variance of the estimates based on the assumption that $\forall i\ \sigma^2(X_i) = 1$.

4.2 Data driven bandwidths: the EBBS algorithm

Since options' data have distribution features (see Section 5) that imply a very careful choice of the bandwidth, the EBBS algorithm was implemented under XploRe to determine the optimal bandwidths.

The basic idea of this algorithm is to estimate the mean square error (MSE) as a function of the bandwidth and then to minimize it at each target point. Hence, at each target point x_l, one bandwidth $h^*_{x_l}$ is selected in a grid $\{h_1, \ldots, h_{max}\}$, so that:

$$MSE\left\{\hat{m}^{(s)}(x_l, h^*_{x_l})\right\} = \min_{h\in\{h_1,\ldots,h_{max}\}} MSE\left\{\hat{m}^{(s)}(x_l, h)\right\}$$

where the MSE is defined by:

$$MSE\left\{\hat{m}^{(s)}(x_l, h)\right\} = \left(bias\left\{\hat{m}^{(s)}(x_l, h)\right\}\right)^2 + \mathrm{Var}\left\{\hat{m}^{(s)}(x_l, h)\right\}. \tag{25}$$

A particularity of this algorithm is that it does not use any asymptotic result. Indeed, EBBS has the following features:

- The variance term used is exact, not asymptotic, but requires an estimate of the conditional variance of the dependent variable given the regressors ($\hat{\sigma}^2(x)$).
- The bias is estimated empirically by calculating $\hat{m}^{(s)}(x; h)$ on a grid of h values and then by modeling the behavior of $\hat{m}^{(s)}(x; h)$ as h varies. Thus, EBBS replaces asymptotic approximations by computation. Remember that $m^{(s)}$ denotes the derivative (s) of order S of the unknown function m in (20).
- One does not need to fit polynomials of degree higher than the degree S of the derivative.

- Contrary to what was written in the last part, this method easily accommodates $p - S$ odd and even.
- Bandwidth selection for estimation of derivatives and when x is multivariate is simple.

From here, X_i denote the standardized regressors, which serve for this algorithm. This standardization is done in order to search for h only on a one–dimensional grid even if $d > 1$. Indeed, at each target point, the bandwidth will be equal in both directions. At the end of the algorithm, the regressors should be de–standardized but the standardization also modify the values of the estimated derivatives and they must also be re–scaled.

$G_x = \{x_l : l \in \mathcal{L}\}$ denotes the grid of target points on $\mathbb{R}^d$ where $\mathcal{L}$ is an index set such that $\mathcal{L} = \{1, \dots, u_1\} \times \cdots \times \{1, \dots, u_d\}$ with $\{u_n\}_{1 \leq n \leq d}$ integers. Remember the difference between a data point X_i, $i = 1, \dots, n$ and a target point x_l, $l \in \mathcal{L}$ and that all expectations are meant to be conditional on $X_1, \dots, X_n$ if not otherwise noted. Hence, bias and variance are conditional expectations.

4.2.1 Estimating the bias

Assume that the bias of $m^{(s)}$ is to be estimated at a target point x_l with a bandwidth h_0. Let $J_b > 1$ be an integer and let $h_0^1, \dots, h_0^{J_b}$ be in a neighborhood of h_0. It is possible to calculate $\hat{m}^{(s)}(x_l; h_0^j)$ for $j = 1, \dots, J_b$. Using these coordinates $\{(h_0^j, \hat{m}^{(s)}(x_l, h_0^j)) : j = 1, \dots, J_b\}$, one can estimate by ordinary least squares the following polynomial:

$$t \geq 1 \quad \hat{m}^{(s)}(x_l; h_0^j) \approx bc_0(x_l) + bc_{p+1-S}(x_l)h^{p+1-S} + \cdots + bc_{p+t-S}(x_l)h^{p+t-S} \quad . \quad (26)$$

where t must be smaller than J_b and the notation bc means bias coefficient. The terms after the intercept in (26) represent the bias and thus the bias is estimated by:

$$bc_{p+1-S}(x_l)h^{p+1-S} + \cdots + bc_{p+t-S}(x_l)h^{p+t-S}. \quad (27)$$

The nature of the bias function in (26) and in (27) is suggested by asymptotics (see Ruppert and Wand (1994) for the case $t = 1$). Asymptotics do not serve for the estimation, they only suggest the model in (26). Ruppert advises to choose $t \geq 2$ in order to prevent problems when $p - S$ is even. Moreover, for estimating the bias at h_0, asymptotics suggest to use only values of h that are greater than h_0.

4.2.2 Estimating the variance

The variance estimation is based on the expression in (24). Let denote here by $\mathcal{X}_l$ the matrix $\mathcal{X}$ in (23) and W_l the matrix W applied to the target point x_l. It is assumed

that $\sigma(X_i) \approx \sigma(x_l)$ for all i such that $K_h(X_i - x_l) \neq 0$ and, if $\sigma(\cdot)$ is continuous, this approximation is increasingly accurate as h tends to 0. Assuming that the column q of $\mathcal{X}_l$ corresponds to the derivative $s = (s_1, \ldots, s_d)$ of order S then combining (23) and (24), one obtains:

$$\mathrm{Var}(\hat{m}^{(s)}(x_l; h)) = \sigma^2(x_l) \left(\prod_{j=1}^{d} (s_j!) \right) \left[(\mathcal{X}_l^\top W_l \mathcal{X}_l)^{-1} (\mathcal{X}_l^\top W_l^2 \mathcal{X}_l) (\mathcal{X}_l^\top W_l \mathcal{X}_l)^{-1} \right]_{qq}. \quad (28)$$

Remember that W_l also depend on h and that therefore each candidate bandwidth yields a different variance estimation.

To evaluate the quantity in (28), one needs to compute before an estimate of $\sigma^2(x_l)$. Ruppert, Wand, Holst and Hössjer (1997) propose an estimation method for these quantities based on the smoothing of squared residuals via EBBS. The first step is to compute a vector of residuals $\hat{u}$ ($\hat{u}_i = Y_i - \hat{m}(X_i, h_m)$) using local polynomials and a global bandwidth h_m. If we assume that the bias of this first smooth is negligible and that $\sigma^2(\cdot)$ is constant in a neighborhood of X_i then $v = [\sigma^2(X_1), \ldots, \sigma^2(X_n)]^\top$ can be estimated through

$$\hat{v} = \frac{S_{h_{EBBS}} \hat{u}^2}{1 + S_{h_{EBBS}} \Delta}$$

where $\Delta = diag\{S_{h_m} S_{h_m}^\top - 2S_{h_m}\}$ and S_{h_m} denotes the smoothing matrix used to estimate $\hat{m} = [\hat{m}(X_1), \ldots, \hat{m}(X_n)]^\top$. The i^{th} row of S_{h_m} corresponds to $e_1^\top (\mathcal{X} W \mathcal{X}) \mathcal{X}^\top W$ with the i^{th} observation as target point. Moreover, $S_{h_{EBBS}}$ denotes the smoothing matrix used to smooth the squared residuals $\hat{u}_i^2$ where the bandwidth is chosen via EBBS. However, to apply EBBS on the squared residuals, there is no need to get a variance function for the residuals. Rather, it is assumed as in Ruppert et al. (1997) that the variance function of the $u_i^2 = \sigma^2(X_i)\varepsilon_i^2$ is proportional to the square of their mean function. Hence, the variance of the squared residuals at a point X_i can be estimated through

$$\widehat{\mathrm{Var}}(u_i^2) = \frac{\widehat{\mathrm{Var}}(\hat{u}_i^2)}{\widehat{\mathrm{E}}(\hat{u}_i^2)^2} (\hat{u}_i^2)^2$$

and remember that

$$\widehat{\mathrm{Var}}(\hat{u}_i^2) = \frac{1}{n} \sum_{i=1}^{n} \hat{u}_i^4 - \left(\frac{1}{n} \sum_{i=1}^{n} \hat{u}_i^2 \right)^2.$$

$\hat{\sigma}^2(x_l)$ can be then obtained by smoothing the $\hat{\sigma}^2(X_i)$ contained in $\hat{v}$ using once again automatically driven bandwidths. However, to compute these estimates $\hat{\sigma}^2(x_l)$, one

needs to apply once EBBS for the n observations which is very expensive in computing time if n is large. Therefore, following an example by Ruppert et al. (1997), the smoothed squared residuals are not corrected by dividing by $(1 + S_{h_{EBBS}}\Delta)$ in the EBBS Quantlet. Rather the variance estimates are obtained directly by smoothing the squared residuals. Note that this degrees of freedom type correction is not sizeable but it increases the variance.

4.2.3 Selecting the bandwidths

Using estimates in (27) and in (28), the $\widehat{MSE}$ is obtained using the relation in (25). As estimating the bias requires J_b fits for each target point x_0 and bandwidth h, some of the fits are reused when calculating the $\widehat{MSE}$ at a nearby bandwidth h_0. Given $G_h = \{h_1, \ldots, h_{max}\}$ the grid of bandwidths, the bias is estimated for h_j using the bandwidths $h_j, \ldots, h_{j+J_b-1}$. Thus, the J_b last values in G_h can not be selected by the EBBS algorithm because no estimate for the bias and MSE are calculated.
Moreover, since the estimate of the mean square error is quite rough as a function of x_l, a smoothed version $\widehat{SMSE}\left\{\hat{m}^{(s)}\left(x_l, h\right)\right\}$ is introduced. In this study, to compute $\widehat{SMSE}$, binomial weights are applied on the η closest points to x_l in G_x. Optimal bandwidths are then chosen at each target point so as to correspond to the first local minimum of the smoothed MSE. The proposed local bandwidth is then:

$$\hat{h}^*(x_l, \eta) = \text{first local} \underset{h \in \{h_1, \ldots, h_{max-J_b}\}}{min} \{\widehat{SMSE}\left\{\hat{m}^{(s)}\left(x_l, h, \eta\right)\right\}\} \tag{29}$$

This local minimum is preferred to a global one since very large values of h tend to greatly underestimate the bias term. Morover, as h increases, the variance of the estimates decrease and thus a global minimum of $\widehat{SMSE}$ would be obtained for h tending to infinity. Finally, the obtained bandwidths are smoothed once again using binomial weights applied on the η_{band} closest points to x_l.
Observe also that if the sample size n is small then it is preferable to use a global bandwidth since a locally varying bandwidth could prove unstable. However, the EBBS algorithm is able to handle this problem. To achieve it, one should smooth the MSE by allocating equal weights to all target points. Then the minimization in (29) should only be performed once.

The EBBS algorithm was implemented under XploRe for d ($d \geq 1$) regressors but only for $p = 1, 2$. This last comment implies that only derivatives of first or second order can be estimated.

```
{f,band} = EBBS(x, y, xgrid, hgrid, OrderDer, p{, msespan
    {, nterms{, bandspan{, varest{, Kernel{, J2{, J1}}}}}}})
```
estimates the unknown function m or one of its derivative via local polynomials and automatically selected bandwidths.

The arguments are `x` a matrix of regressors, `y` the dependent variable, `xgrid` the grid G_x of target points, `hgrid` the grid G_h of bandwidths, `OrderDer` the order (s) of the derivative to be estimated, `p` the order of the polynomial, `msespan` the number (η) of points used to smooth the MSE. Furthermore, `nterms` corresponds to t in (26), `bandspan` is the number (η_{band}) of points to smooth the bandwidth, `varest` is an estimate of the variance at all target points ($\hat{\sigma}^2(x_l)$), Kernel is a string containing the type of Kernel function, `J2` corresponds to J_b which must be larger than `nterms` and `J1` was here set to 0 since to estimate the bias at h_0, only larger bandwidths are used. The output consists of `f` the estimated derivative at all target points in `xgrid` and of `band` the locally selected bandwidths for the standardized data.

5 The data

The dataset was taken from the financial database MD*BASE located at CASE (Center for Applied Statistics and Economics) at Humboldt Universität zu Berlin. Since MD*BASE is a proprietary database, only a limited dataset is provided for demonstration purposes.

This database is filled with options data provided by Eurex. Daily series of 1, 3, 6 and 12 months DM–LIBOR rates taken from the *Thomson Financial Datastream* serve as riskless interest rates. The DAX 30 futures and options settlement data of January 1997 (21 trading days) were used in this study. Daily settlement prices for each option contract are extracted along with contract type, maturity and strike. To compute the interest rates corresponding to the option maturities a linear interpolation between the available rates was performed.

The DAX is a performance index which means that dividends are reinvested. However, using the Black–Scholes model and assuming no dividend yields results in different volatilities for puts and calls contrary to the no–arbitrage assumption contained in the Put–Call parity. This remark can be explained by the fact that until January 2002 domestic investors had an advantage as they may receive a portion or all of the dividend taxes back depending on their tax status. Dividend tax means here the corporate

income tax for distributed gains from the gross dividend. Moreover, observe that the algorithms to extract implied volatilities from option prices are developed in Appendix A.

Since the dividends are rebated to domestic investors the DAX should fall by an amount contained between 0 and these dividend taxes. Indeed, the value of this drop depends on the level of these taxes which may be equal to zero and on the weights of domestic and foreign investors trading the DAX. These dividend taxes have the same effects as ordinary dividends and should therefore be used for computing the implied volatilities and the future price implicit in the Black Scholes formula.

Hafner and Wallmeier (2001) suggest a method in order to get around this problem which consists in computing dividends implied by the Put–Call parity. Indeed, combining the futures pricing formula

$$F_{t,\tau_F} = S_t e^{r_{t,\tau_F}\tau_F} - D_{t,\tau_F}$$

and the Put–Call parity

$$C_t - P_t = S_t - D_{t,\tau_O} - Ke^{-r_{t,\tau_o}\tau_o} \tag{30}$$

we obtain:

$$C_t - P_t = F_{t,\tau_F} e^{-r_{t,\tau_F}} + D_{t,\tau_F,\tau_O} - Ke^{-r_{t,\tau_O}\tau_O} \tag{31}$$

where τ_O is the maturity of the options, τ_F is the maturity of the nearest forward whose volume is positive and $D_{t,\tau_F,\tau_O} = D_{t,\tau_F} - D_{t,\tau_O}$ is the difference between the present values of the dividends. For tick data, it is recommended to use directly the underlying price and (30). However, since no settlement prices are available for the underlying itself, it was necessary to use settlement forward prices.

Using (31), implied dividends were computed for each pair of put and call with the same strike. Theoretically, for a given time to maturity there must be only one value for these implied dividends. Therefore, for each maturity the average of these implied dividends was used to compute the corrected price. Using this method implied volatilities are more reliable as the systematic "gap" which existed before between put and call volatilities disappears. The only uncertainty at this stage is due to the interpolated rates for the maturity τ_O.

For information, the moneyness and maturities of the options are displayed in Figure 1 for January, 3. This figure reveals that the distribution of the maturities and of the strike prices is not uniform at all. Just a few maturities are available and

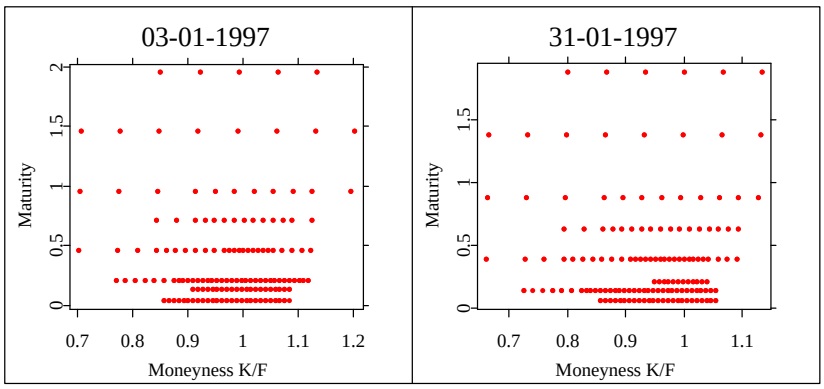

Figure 1: Moneyness and maturities of the options on January 3 and 31, 1997.

there is also a small number of strike prices in order to assure the liquidity of the corresponding options. Furthermore, all series do not have the same range of strikes. In these circumstances, a series whose range is large may provide useful information for the very next series (mainly at boundaries). For example, the first and third series on the left display in Figure 1 are much wider than the second and therefore they may help to estimate the SPD tails of the second cross section of options.

The dataset consists of one file `XFGData9701` with 11 columns. The data can be read into XploRe by loading the quantlib `finance` and then issuing the following command:

```
data=read("XFGData9701.dat")
```

1	Day
2	Month
3	Year
4	Type of option (1 for calls, 0 for puts)
5	Time to maturity (in calendar days)
6	Strike prices
7	Option prices
8	Corrected spot price (implied dividends taken into account)
9	Risk–free interest rate
10	Implied volatility
11	Non–corrected spot price

6 The nonparametric estimates and their reliability

To estimate the SPD corresponding to the maturity of a series of options τ_i, one may use either only this series or the whole sample of options available. Hence, in the first case a univariate regression should be performed on a sample whose size n is strictly smaller than 37 in our dataset. In the second case, the bivariate regression is applied to a sample whose size lies between 144 and 146 depending on the date. The matrix $\mathcal{X}$ in (23) applied to a target point (m_l, τ_l) is then either equal to

$$\mathcal{X}_l = \begin{pmatrix} 1 & M_1 - m_l & (M_1 - m_l)^2 \\ \vdots & \vdots & \vdots \\ 1 & M_n - m_l & (M_n - m_l)^2 \end{pmatrix}$$

or to

$$\mathcal{X}_l = \begin{pmatrix} 1 & M_1 - m_l & \tau_1 - \tau_l & (M_1 - m_l)^2 & (\tau_1 - \tau_l)^2 & (M_1 - m_l)(\tau_1 - \tau_l) \\ \vdots & \vdots & \vdots & \vdots & \vdots & \vdots \\ 1 & M_n - m_l & \tau_n - \tau_l & (M_n - m_l)^2 & (\tau_n - \tau_l)^2 & (M_n - m_l)(\tau_n - \tau_l) \end{pmatrix}.$$

If the goal is to estimate the SPD for a theoretical maturity τ ($\tau \neq \tau_i \ \forall i = 1, \ldots, n$), then only the second framework is allowed. Observe that the moneyness employed in this section is $M = X/F_{t,\tau}$.

6.1 Local versus global bandwidths

Both global and local bandwidths are determined by the EBBS algorithm. To select the optimal global bandwidth, we use the modified version of the EBBS algorithm where the MSE at x_l is smoothed using equal weights at all target points. The parameters serving as input for the EBBS algorithm are as follows:

- The grid $G_h = \{0.35, 0.45, \ldots, 1.25, 1.4, 1.6, 1.8, \ldots, 4, 4.2\}$ contains 25 bandwidths.
- $p = 2$ independently from the derivative order to be estimated.
- The number of terms t in (26) is set to 2.
- Following an advise from Ruppert (1997), the number of bandwidths $J_b + 1$ used to fit the bias is such that $J_b = t$. Thus, the difference between the number of observations and the number of parameter t when we fit the bias model in (26) is 1.

- η the number of points used to smooth the MSE is set to 4.
- The parameter η_{band} is also set to 4.

The grid G_h, the values η and η_{band} are chosen after a rough inspection of the quality of the estimates when bandwidths are selected locally.

First, some remarks concerning the behavior of the bandwidths and of the estimates are presented. In this part, the purpose is to determine if the type of data used (volatility smiles or volatility surfaces) as well as the type of bandwidth have a large influence on the estimates of the quantities V, V' and V'' in (19). Besides, it is of interest to study how the different methods are able to extrapolate outside the sample range.

Figure 2 presents the estimates and optimal bandwidths obtained on January, 3 for a maturity of 14 calendar days when the estimation range is limited to the sample range. The grid of target moneyness goes from 0.85 to 1.1 with a step size of 0.01. Figure 3 shows the same results for a wider range, thus implying extrapolation. Here, the grid goes from 0.7 to 1.3 with a step size of 0.02. On the one hand, Figure 2 reveals that, when no extrapolation is performed, the four different estimates are quiet the same even if the bandwidths differ in type and values. On the other hand, using either the whole surface or the concerned series yields very different out of the sample estimates according to Figure 3. Though the "one series" framework seems to allow a better extrapolation of the observed smile, the estimates based on the "surface" framework may be more meaningful since they include information from near but wider series. Moreover, while, for the whole surface case, the global bandwidth method does not fit the observed data well anymore, the approach using EBBS data driven bandwiths still returns accurate estimates in the sample range. This comment leads to the implementation of the following Quantlet dedicated to fit the implied volatility surfaces using EBBS local bandwidths:

```
{IVsurf,IVpoints} = volsurfEBBS(x, stepwidth, firstXF, lastXF,
    firstMat,lastMat,metric,bandwidthGrid{,global{,IVmethod}})
```

estimates the implied volatility surface $\sigma(m, \tau)$ or $\sigma(K, \tau)$ via local polynomials of order 2 and bandwidths automatically selected via EBBS.

The arguments are `RawData` a matrix containing the forward and strike prices, the interest rates, the maturities, the option prices and the type of option (call or put). The next five input parameters serve to build the grid of maturities and moneyness

(`stepwidth` is a vector containing the step sizes in both directions and `XF` means here moneyness). Furthermore, `metric` allows to choose between the strike price or the moneyness metric. `BandwidthGrid` is the grid G_h in which EBBS selects the bandwidths for the standardized data. If `global` is equal to 1 then the bandwidth selected by EBBS is global else it determines local bandwidths. Finally, `IVmethod` enables the user to choose the algorithm used to compute the Black and Scholes implied volatilities (see Appendix A).

It would be also possible to apply EBBS on tick data but then the second regressor should be the intra–day time t. Therefore, only one option series (one maturity) should serve as input. In Appendix B, an example of the `volsurfEBBS` Quantlet is plotted as well as an example of an intra–day volatility surface.

Regarding the behavior of the bandwidth, the EBBS local bandwidths selected inside the sample boundaries suffer less from extrapolation than the global one. Indeed, the global bandwidth pass from less than 0.8 to 3.8 (the maximum reachable value in G_h) whereas the maximum difference is about 1.4 for local bandwidths. This last increase happens mainly near the sample borders and therefore must be due to the smoothing of the bandwidths.

Figures 4, 5, 6 and 7 present the same graphs for the first and second derivatives of the implied volatility w.r.t. the moneyness. For the first derivative, the same conclusions apply. For the second derivative, it is somewhat different. In fact, in the univariate case, the EBBS algorithm seems to yield unstable estimates of V'', particularly between 0.98 and 1.04. However, as V'' is unknown, it is unclear whether these estimates correspond to the data or not. A solution would be to reduce the step size in the grid of target points and in the grid of bandwidths to get smoother estimates. In practice, it is advocated to first set large step sizes to determine the range in which the local bandwidths are selected and then to decrease the step sizes as well as the range of possible bandwidths according to the first stage.

Another main concern for V'' is the difference between the estimates obtained in the "one series" framework and those based on all available options. To assure that the "one series" framework yields better estimates, the almost linearity of the first derivative confirmed by all estimates may serve as proxy. Indeed, we approximate the global level of the second derivative by computing $\frac{\hat{V}'(1.08)-\hat{V}'(0.86)}{1.08-0.6}$ which is equal to 11.31. Since the estimates based on the largest sample always lie under, we conclude according to the mean value theorem that the bivariate regression does not return good

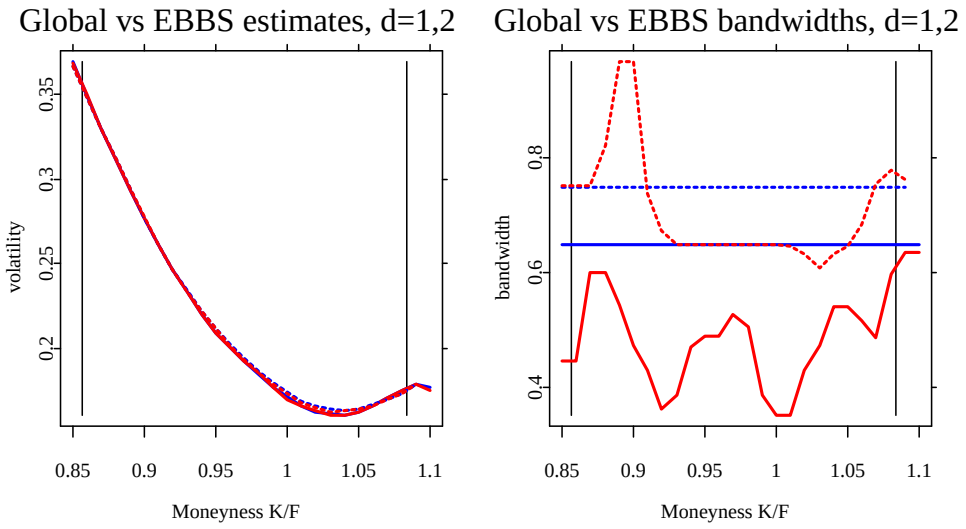

Figure 2: Bandwidths and local polynomial estimates of the the implied volatility smile for both EBBS driven bandwidths (red) and the "optimal" global bandwidth (blue). The dashed lines represent the estimates computed using the whole surface and the plain lines those obtained using the concerned series of options. The black lines surround the sample range.

XFGSPDglobalvsEBBS1.xpl

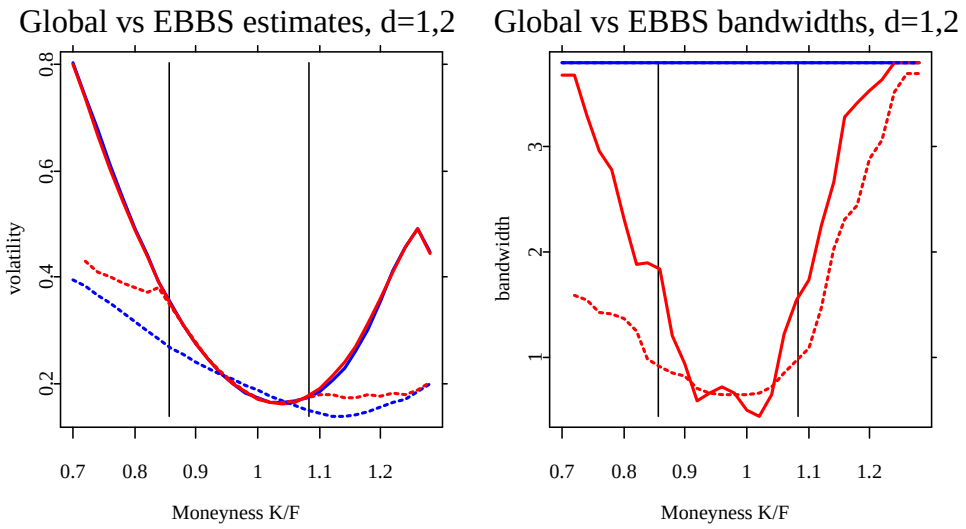

Figure 3: Bandwidths and local polynomial estimates of the the volatility smile for both EBBS driven bandwidths and the "optimal" global bandwidth. The range of estimates is here wider than the sample range which is surrounded by the black lines.

XFGSPDglobalvsEBBS1.xpl

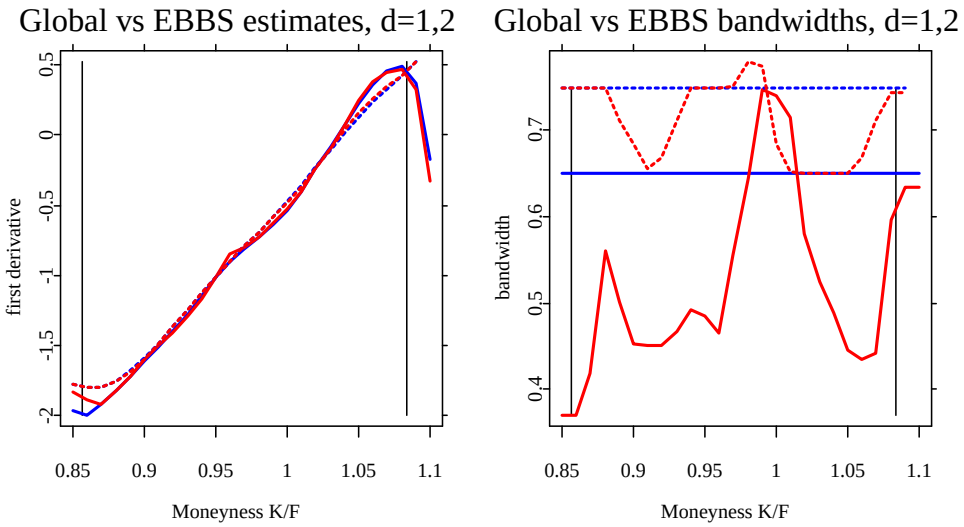

Figure 4: Bandwidths and local polynomial estimates of the the first derivative w.r.t. m of the implied volatility smile for both EBBS driven bandwidths (red) and the "optimal" global bandwidth (blue). The dashed lines represent the estimates computed using the whole surface and the plain lines those obtained using the concerned series of options. The black lines surround the sample range.

XFGSPDglobalvsEBBS3.xpl

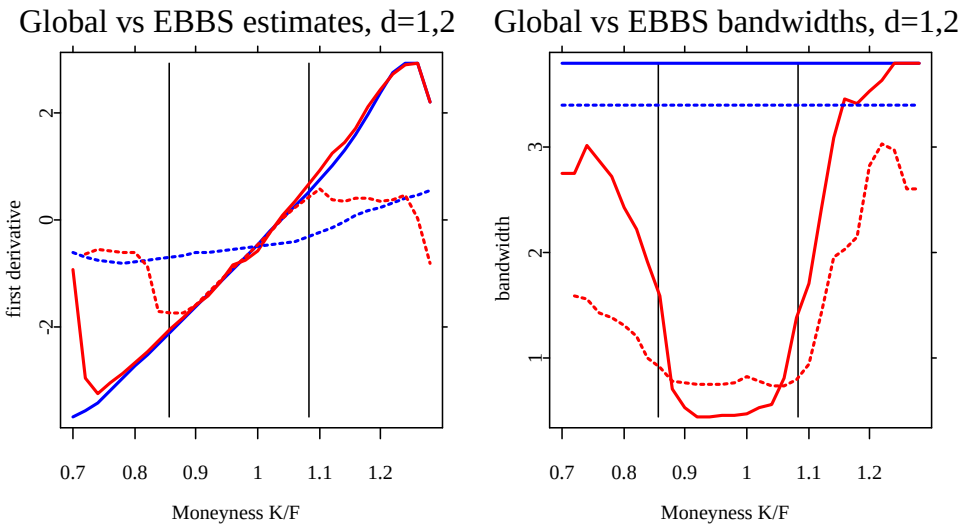

Figure 5: Bandwidths and local polynomial estimates of the the first derivative w.r.t. m of the volatility smile for both EBBS driven bandwidths and the "optimal" global bandwidth. The range of estimates is here wider than the sample range which is surrounded by the black lines.

XFGSPDglobalvsEBBS4.xpl

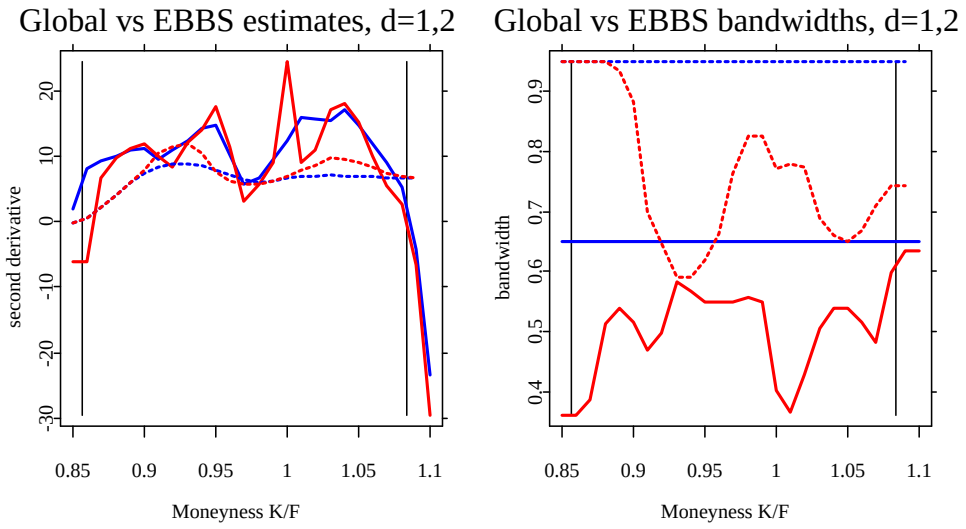

Figure 6: Bandwidths and local polynomial estimates of the the second derivative w.r.t. m of the implied volatility smile for both EBBS driven bandwidths (red) and the "optimal" global bandwidth (blue). The dashed lines represent the estimates computed using the whole surface and the plain lines those obtained using the concerned series of options. The black lines surround the sample range.

XFGSPDglobalvsEBBS5.xpl

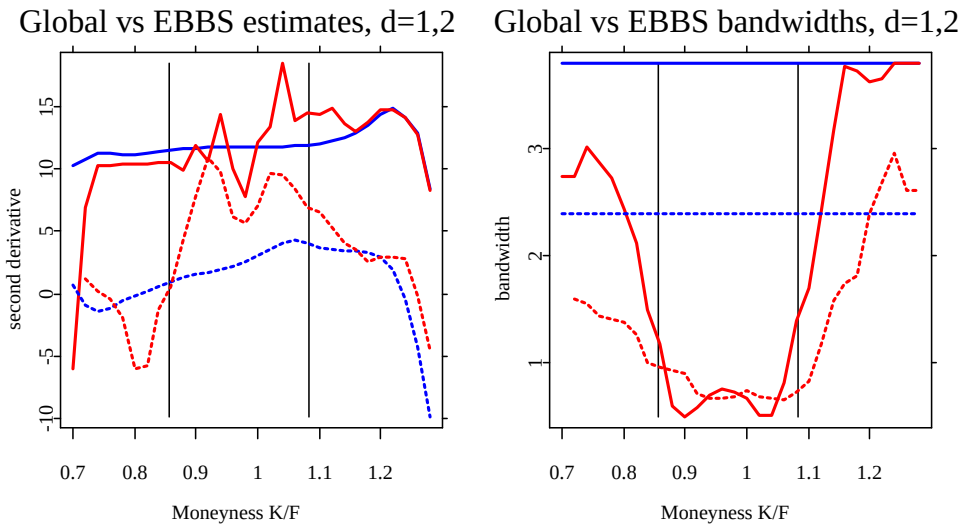

Figure 7: Bandwidths and local polynomial estimates of the the first derivative w.r.t. m of the volatility smile for both EBBS driven bandwidths and the "optimal" global bandwidth. The range of estimates is here wider than the sample range which is surrounded by the black lines.

XFGSPDglobalvsEBBS6.xpl

estimates of the second derivative.

Finally, since EBBS is expensive in computing time, an important concern is the behavior of the global and local bandwidths towards the order (S) of the derivative. Actually, it would be worthwhile in term of computing time to only apply EBBS once to fit V and then to reuse the same bandwidths when estimating V' and V''. To test the feasibility of this method, we estimate V' and V'' using the bandwidths h_V selected for V. These quantities $\hat{V}'_{h_V}$ and $\hat{V}''_{h_V}$ are then substract from the estimates $\hat{V}'_{h_{V'}}$ and $\hat{V}'_{h_{V''}}$ already displayed in figures 4, 5, 6 and 7. These differences are visible on figures 8 and 9. In all cases, using the bandwidth h_V to estimate the first derivative V' does not seem to be a problem since the values are very small in comparison with the niveau of V'. On the other hand, using h_V to fit V'' returns estimates significantly different than those obtained when applying directly EBBS to V''. However, it does not happen in the univariate case with h_V global. Indeed, in this last case, the difference is always equal to 0.

Linking all these observations, it seems that the best solution is to use the optimal global bandwidth within the smile framework. Indeed, this solution yields stable and meaningful estimates of the second derivative and the EBBS algorithm may be applied only once. Nevertheless, if the SPD corresponds to a theoretical maturity τ, the surface framework is required and then it is recommended to use local bandwidths since the global bandwidth produces strong underestimates of the second derivative V'' and simply fails when extrapolating out of the sample range. The same conclusions hold for different maturities (see Appendix C).

From the statistical point of view, we have suggested one optimal method for each framework (theoretical or existing maturity). However, it is also possible to test the reliability of the estimates through financial criteria.

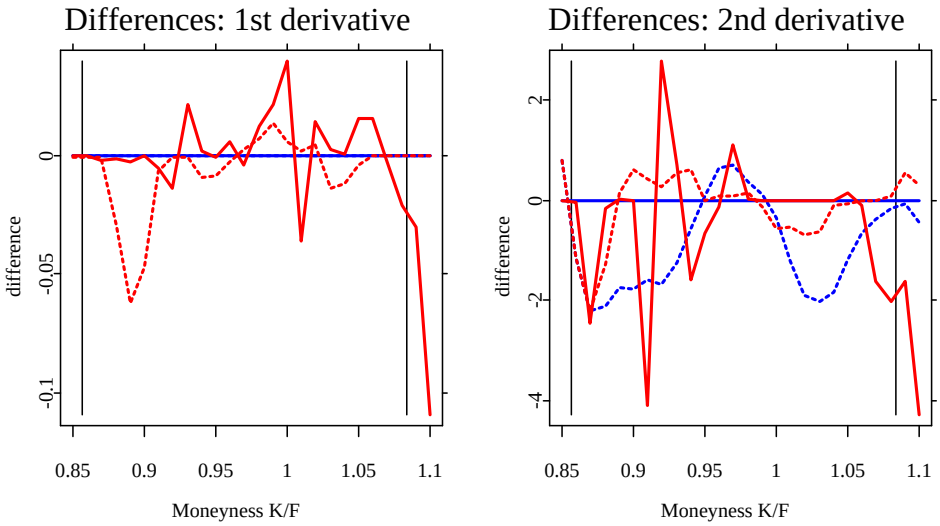

Figure 8: On the left display, the difference between $\hat{V}'_{h_{V'}}$ and $\hat{V}'_{h_V}$. On the right display, the difference between $\hat{V}''_{h_{V''}}$ and $\hat{V}''_{h_V}$. The grid of target points is here restricted to the sample range. The lines have the same meaning as in the previous displays.

XFGSPDglobalvsEBBS7.xpl

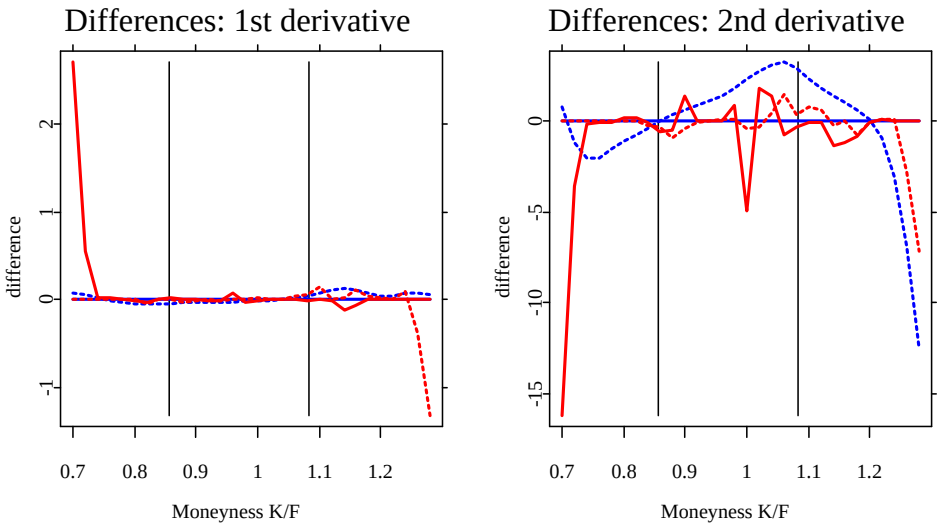

Figure 9: On the left display, the difference between $\hat{V}'_{h_{V'}}$ and $\hat{V}'_{h_V}$. On the right display, the difference between $\hat{V}''_{h_{V''}}$ and $\hat{V}''_{h_V}$. The grid of target points goes from 0.7 to 1.28.

6.2 Constraints on the monotonicity and convexity of Option Pricing Functions

Aït–Sahalia and Duarte (2001) introduce a local polynomial estimation with shape restrictions to avoid any violation of constraints imposed by the no–arbitrage theory. Indeed, the no–arbitrage assumption requires that the call pricing function is a decreasing and convex function of the option strike price K. This sentence can be summarized by the following inequalities:

$$\begin{cases} \frac{\partial C(S_t,K,\tau,r_{t,\tau},\delta_{t,\tau})}{\partial K} \leq 0 \\ \frac{\partial^2 C(S_t,K,\tau,r_{t,\tau},\delta_{t,\tau})}{\partial K^2} \geq 0 \end{cases} \tag{32}$$

Moreover, setting the call payoff ($Z(S_T) = max(S_T - K, 0)$) into equation (1) and taking the first derivative w.r.t. K results in:

$$\frac{\partial C(S_t, K, \tau, r_{t,\tau}, \delta_{t,\tau})}{\partial K} = -e^{-r_{t,\tau}\tau} \int_K^\infty f_t^*(S_T) dS_T$$

As f_t^* is a density, its integral must be smaller than one and therefore, we get a bounded interval for the first derivative of the call pricing function w.r.t. the strike price:

$$-e^{-r_{t,\tau}\tau} \leq \frac{\partial C(S_t, K, \tau, r_{t,\tau}, \delta_{t,\tau})}{\partial K} \leq 0. \tag{33}$$

In addition to the constraints in (32) and (33), we consider that if the integral of the density is larger than 1, our method fails. Thus, to verify the reliability of the method presented here, an experiment, which aims at testing these constraints, was lead in the following way:

- get all options and their features for one day
- build a strike (or moneyness) grid common to all days (in our case, the grid goes eiter from 2300 to 3250 or from 2500 to 3125.)
- estimate the implied volatility and its first two derivatives on this grid using the extracted options and the EBBS algorithm.
- use the derivations from Section 3.2 to compute the SPD and the first and second derivatives of the call pricing function with respect to K.
- compute the integral of the SPD via Riemann sums
- test if the constraints are violated
- repeat this for all maturities and all days

These tests are performed for two different grids, one inside the sample borders and one larger. The second case is done to evaluate the possible problems coming from extrapolation. Besides, this task is done for both global and local bandwidths, and using either the whole surface or the concerned smile. The results of these tests are exposed respectively in the tables 1 and 2.

	Smile framework		Surface framework	
Option series	Global	EBBS	Global	EBBS
First maturity	15 (11,0,10,4)	18 (11,15,0,4)	2 (2,0,1,0)	2 (1,0,1,1)
Second maturity	1 (1,0,0,0)	2 (2,0,0,0)	0	0
Third maturity	10 (10,0,8,0)	10 (10,0,10,0)	1 (0,0,1,0)	1 (0,0,1,0)
Other series	0	0	0	0

Table 1: Number of days of January, 1997 where the constraints are violated. These values are obtained for a grid going from 2600 to 3125. The numbers in brackets represent respectively the number of days where the following constraints are violated (lower bound in (33), upper bound in (33), second inequality in (32), constraint on the integral of the SPD). Notice that the non-parametric estimates presented in 6.1 (January 3) strangely never violate the constraints.

	Smile framework		Surface framework	
Option series	Global	EBBS	Global	EBBS
First maturity	18 (14,2,6,10)	18 (14,2,13,10)	3 (2,0,1,2)	4 (2,1,1,1)
Second maturity	8 (3,0,4,2)	15 (7,1,7,3)	1 (0,0,1,0)	3 (0,0,2,1)
Third maturity	11 (10,0,10,1)	15 (10,0,15,1)	4 (0,0,4,1)	4 (0,0,4,0)
Fourth maturity	5 (0,0,5,0)	5 (0,0,5,0)	0	0
Other series	0	0	0	0

Table 2: Number of days of January, 1997 where the constraints are not fulfilled. These values are obtained for a grid going from 2300 to 3250. The brackets have the same meaning as in Table 1.

The first point to notice is that the first derivative of the call pricing function C with

respect to K does not depend on the second derivative V'' (see Section 3.2). Since the constraints involving this first derivative are often violated, it is not possible to accuse only the inaccurate or unstable estimates $\hat{V}''$. Secondly, extrapolating outside the range has a large influence since passing from the first grid to the larger one always increases the number of days where the constraints are violated. Moreover, the 10 failures observed for the third series in table 1 happen after the third Friday of January. These violations are then due to the extrapolation since the third series is after this date very narrow, see the width of the concerned series on the right display of figure 1. These observations confirm the approach developped by Aït–Sahalia and Duarte (2001) when estimating SPD for small maturities or when extrapolation is desired.

Furthermore, the choice to use the global bandwidth in the univariate case is confirmed since it implies always less violated constraints than in the local bandwidth case. However, using the whole sample implies less violated constraints. Therefore, there is a trade off between the quality of the nonparametric estimates and the fulfillment of the no–arbitrage constraints.

At this stage, we have shown that it is necessary to keep a critical eye on the nonparametric and SPD estimates, particularly when the maturity is small or when the SPDs are based on out of the sample estimates. Another financial approach regards the accuracy of the different SPD estimates to replicate the observed prices.

6.3 Best estimates by comparing theoretical and observed prices

The quality of the different nonparametric estimates are here compared through the prices that their resulting SPDs yield. Since we have shown that extrapolating outside the range may cause the violation of no–arbitrage constraints, it is inadequate to determine prices from contingent claims whose payoffs are positive ouside the available strike range. Therefore, using butterfly spreads defined in section 2.1 is preferable to simply compute the call or put prices. The theoretical prices presented here are based on equation (1) and on the butterfly payoff in (4).

The method performed rely on a cross–validation procedure. Thus, we remove from the sample the three calls used to calculate the observed butterfly prices before estimating the SPD. The butterfly spreads are centered on $K = 2875$ and their width $2\Delta K$ is set to 200. Hence, they do not move with the moneyness but are always inside

the sample range. To calculate the integral in (1), Riemann sums are built on a grid containing $2\Delta K$ target points. The grid space is then equal to 1. Table 3 points out for the first available maturity the results in term of the relative pricing error E:

$$E = \frac{P_{observed} - P_{SPD}}{P_{observed}}$$

where $P_{observed}$ is the observed price of the butterfly spread and P_{SPD} is the price computed using the SPD estimate and (1). The mean of absolute values of the pricing errors confirm that the univariate regression is advocated when considering an existing maturity τ_i. These results also reveal that the locally selected bandwidths yield more often better estimates of the observed price. However, the difference in the univariate case is not sufficiant to change the previous decision and use locally driven bandwidths. Therefore, in the following, the univariate regression is always performed with the EBBS global bandwidth and the bivariate with locally driven bandwidths.

Moreover, the violated constraints observed for the first maturity in the last section may not be due to the estimation method but rather may be already present in the settlement data. Thus, to confirm this statement, it would be interesting to redo the same constraint tests using tick data. In the following section, we present the SPDs, deltas and gammas estimates.

Date	Smile		Surfaces	
	Global	EBBS	Global	EBBS
January, 3	-6.5	-5.5	-15.5	-14
January, 6	4.2	3.9	-2.4	-0.2
January, 7	-7.1	-3.8	-18.7	-15.2
January, 8	-18.1	-18.2	-32.9	-28.2
January, 9	-15	-14.9	-30.7	-22.9
January, 10	5.3	5.2	-10.1	-0.7
January, 13	7.7	6.2	7.6	6.8
January, 14	-3.5	-4	-2.9	-4.6
January, 15	-28	-27.4	-32.9	-32.3
January, 16	9.8	9.4	1.6	4
January, 17	8.4	9.5	8.8	8.75
January, 20	3.4	4.1	3.4	3.6
January, 21	-0.5	-0.4	1.1	0.4
January, 22	-12.9	-6.8	-6.9	-6.3
January, 23	-8.1	-7.2	-8.9	-7.3
January, 24	-1.1	-1.9	-0.9	-0.9
January, 27	-1	-0.4	1.3	1.4
January, 28	2.3	2	-1.15	-8.4
January, 29	2.0	1.4	6.8	6.6
January, 30	-0.2	-0.1	-4.2	-1.2
January, 31	1	0.4	5.8	6.7
Mean	-2.76	-2.32	-6.78	-4.95
Mean of absolute values	6.95	6.33	10.24	8.59

Table 3: Pricing errors E in percent for butterfly spreads with a central strike of 2875 and $\Delta K = 100$. The observed price is computed using the series of options whose maturity decreases from 77 to 49 during the period. The theoretical price is computed for the corresponding maturity.

7 SPD estimates and confidence bands

7.1 State price density, delta and gamma estimates

A Quantlet to estimate the SPD via local polynomials has been implemented under XploRe for d ($d = 1, 2$). It allows all the possibilities exposed in the last section. For instance, one may use one or all series of options. Moreover, it is possible to choose between locally and globally driven bandwidths or input your own bandwidths.

```
{fstar,delta,gamma,band} = SPDlp(RawData, xGrid, locband,
    metric{, spdMaturity, IR, ForwardPrice})
    estimates the SPD using either only one smile (σ(M) or σ(K)) or the whole volatiliy
    surface (σ(M,τ) or σ(K,τ)).
```

The arguments are `RawData` a matrix containing the forward and strike prices, the interest rates, the maturities, the option prices and the type of option (call or put). `xgrid` is the grid of target points which should depend from the `metric` chosen. Indeed, it is possible to get the SPD on a strike price metric or on a moneyness metric ($m = S_T/F_{t,\tau}$). `locband` is a vector of bandwiths. If `locband` is set to 0 then the EBBS algorithm determines local bandwidths in a predefined grid. If it is set to -1, it determines an optimal global bandwidth. The three last parameters are required only if the input data include more than one series of options. Then, it is necessary to give the maturity (`spdMaturity`) for which the SPD should be computed and the corresponding interest rate (`IR`) and forward price (`ForwardPrice`). The output consists of the SPD (`fstar`), the hedging parameters (`delta` and `gamma`) and the bandwiths at each target point.

Here, some first features of the SPD are presented. The estimates are in the univariate case based on the optimal global bandwidth and in the bivariate on locally driven bandwidths.

First, a graphical comparison between the semiparametric and the Black & Scholes SPDs is presented. In fact, the main purpose is to see whether both SPDs really differ. To compute the Black & Scholes SPD, the volatility parameter σ_{BS} is equal to the observed ATM implied volatility. The two optimal semiparametric SPDs are plotted (one for the univariate and one for the bivariate case) and $\sigma_{BS} = 0.1694$ is computed using the two nearest calls and puts. In Figures 10 and 11 the three SPDs are respectively plotted for a maturity of 14 and 49 days. The same results as in Aït–

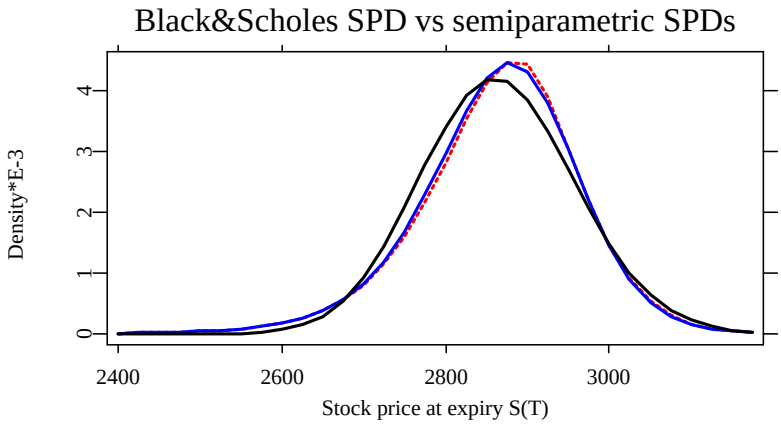

Figure 10: The Black & Scholes SPD (black) and the semiparametric SPD (red and blue) corresponding to a maturity of 14 days on January, 3. The colors and styles of the semiparametric SPDs have the same meaning as in Section 6.1.

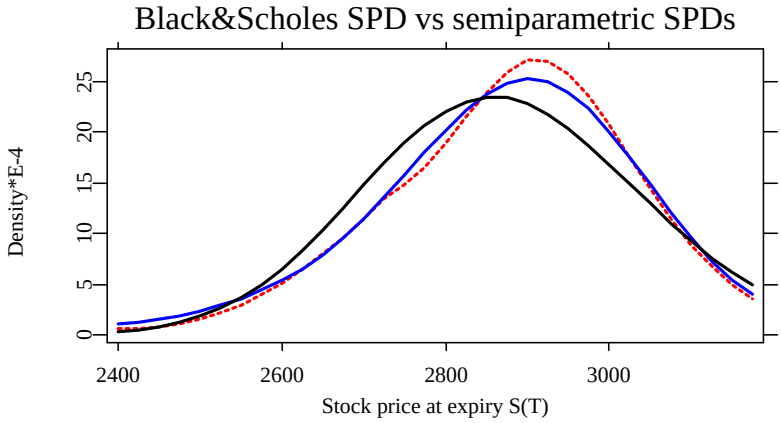

Figure 11: The Black & Scholes SPD (black) and the semiparametric SPD (red and blue) corresponding to a maturity of 49 days on January, 3. The colors and styles of the semiparametric SPDs have the same meaning as in Section 6.1.

XFGSPDbsVSsp.xpl

Sahalia and Lo (1998) concerning the difference between the semiparametric and the Black & Scholes SPDs are illustrated. For example, the semiparametric SPDs exhibit a negative skewness and an higher kurtosis than the parametric one. Thus, using the local polynomial estimators one captures the effect of the "volatility smile" and its

effects on the higher moments such as skewness and kurtosis. However, the second graph reveals visible differences between our both estimates. Indeed, the SPD based on the whole sample (blue, dashed) seems to have an higher kurtosis which may be explained by the influence of the first option series on our estimates of the second SPD. Since it was found that the univariate case allows a better track of observed prices situated near the ATM point, we can assume that the red line is nearer to the true value than the blue one.

It is now of interest to illustrate the pattern followed by the SPDs when the maturity increases. `XFGSPDoneday.xpl` calculates and plots the local polynomial SPDs for January 10, 1997 for different theoretical times to maturity ($\tau = 0.125, 0.25, 0.375$). Hence, here the bivariate framework is used. The SPDs are finally displayed in Figure 12. This figure shows the expected effect of time to maturity on the SPD, which is

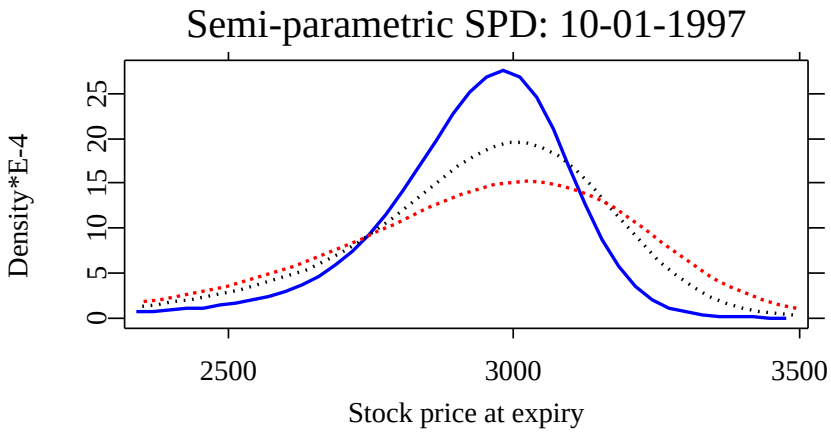

Figure 12: Local Polynomial SPD for $\tau = 0.125$ (blue,filled), $\tau = 0.25$ (black,dashed) and $\tau = 0.375$ (red,dotted).

`XFGSPDoneday.xpl`

an increase of variance and a loss of kurtosis. This effect on the kurtosis was confirmed by computation. Figure 13 and Figure 14 show Delta and Gamma for the full range of strikes and for the three same theoretical maturities. This method allows the user to get in one step the SPD and both greeks for all strikes and maturities.

A natural question that may arise is how do the SPDs evolve over time. In this section an illustrative example is used to show the dynamics of the SPD over the month of January 1997. `XFGSPDonemonth.xpl` estimates the SPD for each trading day in January 1997 and plots it in three–dimensional space. The x–axis is the moneyness,

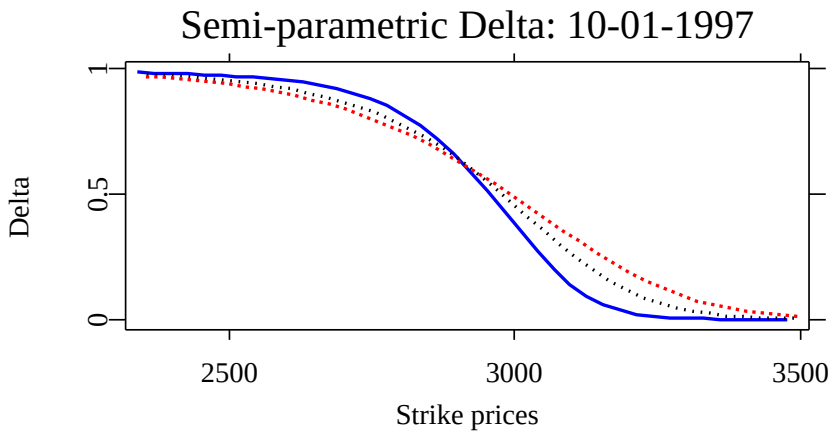

Figure 13: Local Polynomial Delta for $\tau = 0.125$ (blue,filled), $\tau = 0.25$ (black,dashed) and $\tau = 0.375$ (red,dotted).

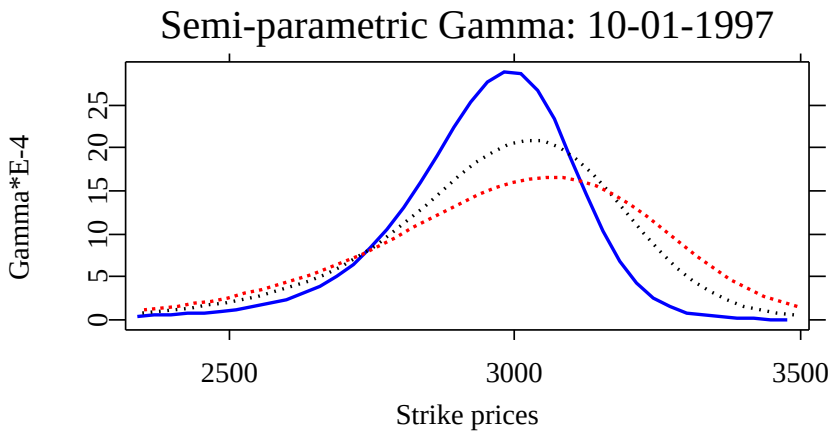

Figure 14: Local Polynomial Gamma for $\tau = 0.125$ (blue,filled), $\tau = 0.25$ (black,dashed) and $\tau = 0.375$ (red,dotted).

XFGSPDoneday.xpl

y–axis is the trading day, and the z–axis is the SPD.

Figure 15 shows the local polynomial SPD for the three first weeks of January, 1997.

7.2 Bootstrap confidence bands

The method using the derivations in Section 3.2 serves to estimate the SPD, where V, V' and V'' from (19) are computed via local polynomials and the EBBS global bandwidth. The method is here based on the univariate regressions.

With a polynomial of order $p = 2$ and a bandwidth $h = \left(n^{-1/9}\right)$, it can be shown that

$$E|\hat{f}_n^* - f^*|^2 = \mathcal{O}\left(n^{-4/9}\right),$$

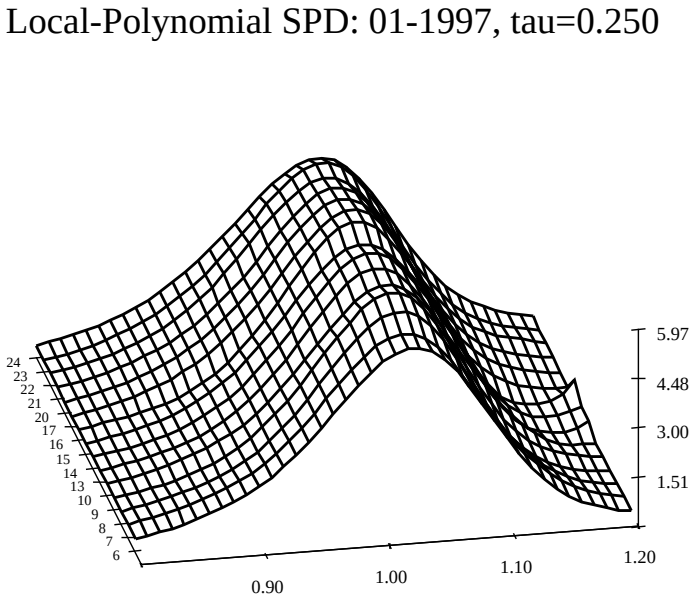

Figure 15: Three weeks State–Price Densities on a moneyness scale.

XFGSPDonemonth.xpl

because

$$
\begin{aligned}
E|\hat{V}_n - V|^2 &= \mathcal{O}\left(n^{-8/9}\right), \\
E|\hat{V}_n' - V'|^2 &= \mathcal{O}\left(n^{-4/9}\right), \\
E|\hat{V}_n'' - V''|^2 &= \mathcal{O}\left(n^{-4/9}\right).
\end{aligned}
$$

This result can be obtained using some theorems related to local polynomial estimation, for example in Fan and Gijbels (1996), if some bound conditions are satisfied.

An asymptotic approximation of $\hat{f}_n^*$ is complicated by the fact that $\hat{f}_n^*$ is a non linear function of V, V' and V''. Analytical confidence intervals can be obtained using delta methods proposed by Aït–Sahalia (1996). However, an alternative method is to use the bootstrap to construct confidence bands. The idea for estimating the bootstrap bands is to approximate the distribution of

$$\sup_k |\hat{f}^*(k) - f^*(k)|.$$

The following procedure illustrates how to construct bootstrap confidence bands for local polynomial SPD estimation.

1. Collect daily option prices from MD*BASE, only choose those options with the same expiration date, for example, those with time to maturity 49 days on Jan 3, 1997.

2. Use the local polynomial estimation method to obtain the empirical SPD. Notice that when τ is fixed the forward price F is also fixed. So that the implied volatility function $\sigma(K/F)$ can be considered as a fixed design situation, where K is the strike price.

3. Obtain the confidence band using the wild bootstrap method. The wild bootstrap method entails:

   - Suppose that the regression model for the implied volatility function $\sigma(K/F)$ is:
   $$Y_i = \sigma\left(\frac{K_i}{F}\right) + \varepsilon_i, \quad i = 1, \cdots, n.$$
   - Choose a bandwidth g which is larger than the optimal h in order to have oversmoothing. Estimate the implied volatility function $\sigma(K/F)$ nonparametrically and then calculate the residual errors:
   $$\tilde{\varepsilon}_i = Y_i - \hat{\sigma}_h\left(\frac{K_i}{F}\right).$$
   - Replicate B times the series of the $\{\tilde{\varepsilon}_i\}$ with wild bootstrap obtaining $\{\varepsilon_i^{*,j}\}$ for $j = 1, \cdots, B$, Härdle (1990), and build B new bootstrapped samples:
   $$Y_i^{*,j} = \hat{\sigma}_g\left(\frac{K_i}{F}\right) + \varepsilon_i^{*,j}.$$
   - Estimate the SPD $f^{*,j}$ using bootstrap samples, Rookley's method and the bandwidth h, and build the statistics
   $$T_f^* = \sup_z |f^{*,j}(z) - \hat{f}^*(z)|.$$
   - Form the $(1-\alpha)$ bands $[\hat{f}^*(z) - t_{f^*,1-\alpha},\ \hat{f}^*(z) + t_{f^*,1-\alpha}]$, where $t_{f^*,1-\alpha}$ denotes the empirical $(1-\alpha)$-quantile of T_f^*.

Two SPDs (Jan 3 and Jan 31, 1997) whose times to maturity are 49 days were estimated and are plotted in Figure 16. The bootstrap confidence band corresponding to the first SPD (Jan 3) is also visible on the chart. In Figure 17, the SPDs are plotted on a moneyness metric. It seems that the differences between the SPDs can

be eliminated by switching to the moneyness metric. Indeed, as can be extracted from Figure 17, both SPDs lie within the 95 percent confidence bands. The number of bootstrap samples is set to $B = 100$. The local polynomial estimation was done on standardized data, h is then set to 0.75 for both plots and g is equal to $1.1h$. The bandwidth h value is the maximum of both optimal global bandwidths. Indeed, the series concerned is not the same on January 3 and 31 and therefore the optimal selected bandwidth is different. Notice that greater values of g are tried and the conclusion is that the confidence bands are stable to an increase of g.

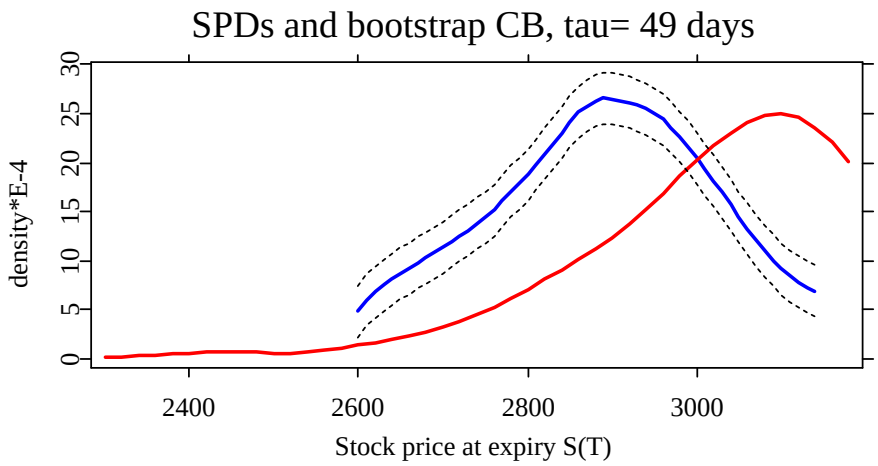

Figure 16: SPD estimation and bootstrap confidence band. The blue line represents the SPD on January 3 and the red line the SPD on January 31.

XFGSPDcb.xpl

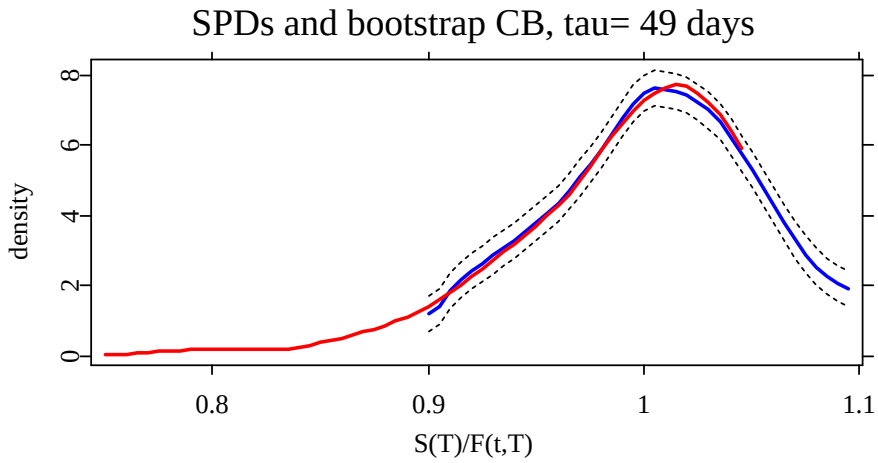

Figure 17: SPD estimation and bootstrap confidence band (moneyness metric).

XFGSPDcb2.xpl

8 Comparison to Implied Binomial Trees

In Chapter 7 of Härdle et al. (2002), the Implied Binomial Trees (IBT) are discussed. This method is a close approach to estimate the SPD. It also recovers the SPD nonparametrically from market option prices and uses the Black Scholes formula to establish the relationship between the option prices and implied volatilities as in Rookely's method. In Härdle et al. (2002), the Black Scholes formula is only used for Barle and Cakici IBT procedure, but the CRR binomial tree method used by Derman and Kani (1994) has no large difference with it in nature. However, IBT and nonparametric regression methods have some differences caused by different modelling strategies.

The IBT method might be less data–intensive than the nonparametric regression method. By construction, it only requires one cross section of prices. In the earlier application with DAX data, option prices are used with different times to maturity for one day to estimate the implied volatility surface first in order to construct the tree using the relation formula between option prices and risk–neutral probabilities. The precision of the SPD estimation using IBT is heavily affected by the quality of the implied volatility surface and the choice of the levels of the implied tree. Furthermore, from the IBT method only risk–neutral probabilities are obtained. They can be considered as a discrete estimation of the SPD. However, the IBT method is not only useful for estimating SPD, but also for giving a discrete approximation of the underlying process.

The greatest difference between IBTs and nonparametric regression is the requirement of smoothness. The precision of Rookley's SPD estimation is highly dependent on the selected bandwidth. Even if very limited option prices are given, a part of the SPD estimation still can be obtained using nonparametric regression, while the IBT construction has to be given up if no further structure is invoked on the volatility surface. Rookley's method has on first sight no obvious difference with Aït–Sahalia's method theoretically, Aït–Sahalia and Lo (1998). But investigating the convergence rate of the SPD estimation using Aït–Sahalia's method allows one to conduct statistical inference such as test of the stability of the SPD and tests of risk neutrality.

The quantlet `XFGSPDcom.xpl` shows a comparison of the SPD estimates by IBT and Rookley's methods. The differences between these two SPD estimates may be due to the selection of the bandwidths in Rookley's method, the choice of steps in the construction of the IBT and the use of DAX implied dividends in Rookley's method. Figure 18 shows the implied binomial trees and the local polynomial SPDs for Jan-

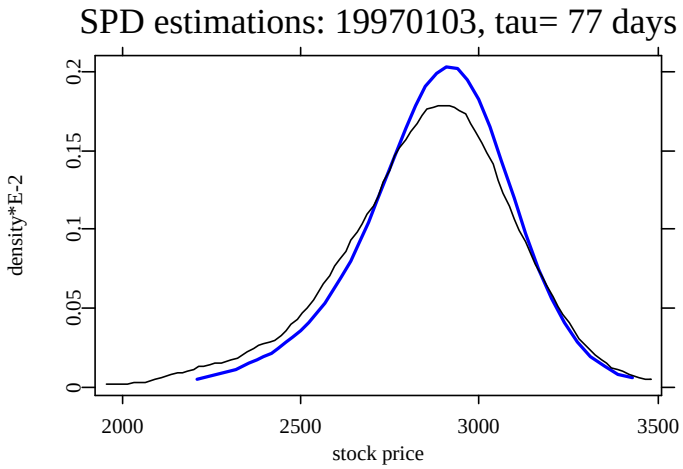

Figure 18: Comparison of different SPD estimations, by Rookley's method (blue) and IBT (black,thin).

XFGSPDcom.xpl

uary, 3 1997. The local polynomial SPD is here determined using the optimal global bandwith and the univariate regression.

Both densities seems to be quiet different. Indeed, the IBTs SPD shows a fatter left tail than the Rookley's one and the Rookley's SPD shows a larger kurtosis. The cross–validation procedure presented in 6.3 serves here again. However, since the largest difference between both SPDs is observed at the ATM point (see Figure 18), the test is nolonger applied to a butterfly spread with a fix center but rather we build two butterfly spreads whose centers surround the ATM point. Hence, the centers of the butterfly spread follow the forward price movement. The width $2\Delta K$ is chosen as in 6.3 equal to 200.

This procedure is done for the 21 days of January 1997. Figures 19 and 20 show the results in term of relative pricing error E defined in section 6.3. It seems that both SPDs have a too small kurtosis since the observed prices of butterfly spreads are larger than those of both SPDs in most of the cases. However, Rookley's SPD is in mean nearer to the observed price than the IBT's one.

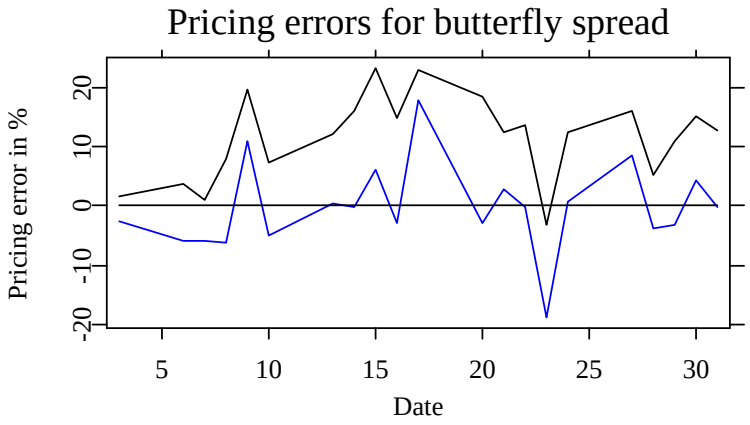

Figure 19: Relative pricing error for the butterfly spread centered on the nearest strike on the left side of the ATM point. The black lines represent the IBT's pricing errors and the blue the Rookley's errors.

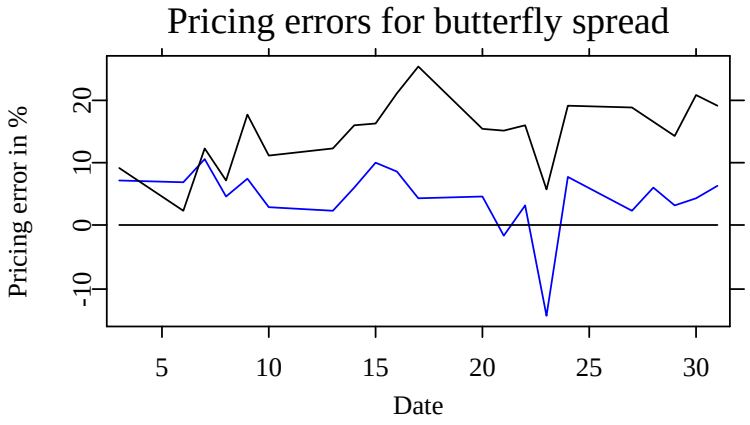

Figure 20: Relative pricing error for the butterfly spread centered on the nearest strike on the right side of the ATM point.

9 Conclusion

In this study, a semiparametric approach to estimate state price densities is presented and investigated. The semiparametric model requires the estimation of the implied volatility smile and its two first derivatives. Therefore, the local polynomial method is introduced since it is able to provide nonparametric estimates of an unknown function and of its derivatives. However, this method is mainly driven by the smoothing parameter also called bandwidth, which may be determined either by plug–in rules or data–based selectors. Since the data sample covers only discretely the strike and maturity dimension within a limited range, the bandwidth selection is the key issue in this study. Hence, we implement the Empirical Bias–Bandwidth Selector of Ruppert (1997) which has the nice feature to select automatically either global or local bandwidths, both optimal in the sense of the mean square error. Normally, the local selection should be preferred but we show that the global bandwidth method has some advantages (stability for example) compared to the method using local bandwidths when the sample size is small.

Once the nonparametric estimates are obtained, it is then possible to compute the SPDs and the hedging parameters for the whole range of strike prices. On the one hand, our method is able to estimate the SPDs for theoretical and existing maturities. The theoretical case is obtained using options with different maturities and by applying the local polynomials on the implied volatility surface. On the other hand, the nonparametric estimates often imply the violation of different no–arbitrage constraints and therefore one should keep a critical eye on the estimates and on the settlement prices which may already contain these no–arbitrage violations. The method of Aït–Sahalia and Duarte (2001) should be able to handle this problem. Moreover, our method was proved to be more accurate than the implied binomial trees to estimate the SPDs.

Appendix

A Computation of implied volatilities

As an option is a right and not an obligation, its price is an increasing function of the volatility parameter. Thus, due to this monotony, there is a bijection between the option price and its volatility, i.e. to each option price corresponds one unique volatility. Therefore, instead of calculating the option price as a function of its volatility, it is possible to compute the volatility implied by the theoretical price of the option. As the study is based on European options, the theoretical price is computed using the Black-Scholes model, briefly presented in Section 2.2. In the case of American options, the price is based on the so called binomial trees.

However, there is no analytical formula to determine the implied volatility according to its option price. Thus, algorithms to find nonlinear equation roots are necessary but as the price is an increasing function, these algorithms are simplified. The two main algorithms for this purpose are:

- the bisection method
- the Newton–Raphson algorithm

The Newton–Raphson algorithm is advocated as its rate of convergence is quadratic. Applied to the computation of the implied volatility, an iteration of the Newton–Raphson algorithm has the following form:

$$\sigma_{n+1} = \sigma_n - \frac{P_{BS}(S_t, K, \tau, r_{t,\tau}, \delta_{t,\tau}, \sigma_n) - P_{observed}}{\left.\frac{\partial P(\cdot)}{\partial \sigma}\right|_{\sigma=\sigma_n}}$$

where $P_{BS}(\cdot)$ denotes the Black–Scholes option price, $P_{observed}$ is the option price observed on the market and σ_n is the n^{th} iteration of σ.

The choice of the first value σ_0 is essential to assure the convergence of the algorithm. Manaster and Koehler (1982) propose to choose σ_0 so that it maximizes the vega($\frac{\partial P(\cdot)}{\partial \sigma}$) of the option. The vega of European options is the same for puts and calls and is equal to:

$$\forall \sigma : \Lambda_{call} = \Lambda_{put} = \frac{S_t \sqrt{\tau} e^{-\frac{d_1^2}{2}}}{\sqrt{2\pi}} > 0$$

and the second derivative with respect to the volatility is

$$\frac{\partial^2 P(\cdot)}{\partial \sigma^2} = \frac{S_t \sqrt{\tau} d_1 d_2 e^{-\frac{d_1^2}{2}}}{\sqrt{2\pi}} \geq 0.$$

where d_1 and d_2 are defined in Section 2.2.

Therefore, the critical points are obtained for $d_1 = 0$ and $d_2 = 0$ which implies that $\sigma^2 = -2\frac{ln(S/X)+r\tau}{\tau}$ and $\sigma^2 = 2\frac{ln(S/X)+r\tau}{\tau}$. For those both values, the second derivative of vega with respect to the volatility ($\frac{\partial^3 P(\cdot)}{\partial \sigma^3}$) is negative assuring that those points are maxima. Thus, the start value of the Newton–Raphson algorithm can be set equal to:

$$\sigma_0 = \sqrt{\frac{2}{\tau}\left|ln\left(\frac{S}{X}\right) + r\tau\right|}$$

Manaster and Koehler (1982) show that in this case, the series $\{\sigma_n\}$ is monotonic and bounded and therefore converges to the true value. The Quantlet `ImplVola` computes in XploRe implied volatilities for European options, giving the choice between both algorithms.

B Implied volatility surfaces

As example of the `volsurfEBBS` Quantlet dedicated to the implied volatility surface, one display is presented for the implied volatility surface ($\sigma(m, \tau)$). For demonstration purpose, an intra–day surface ($\sigma(m, t)$) is .

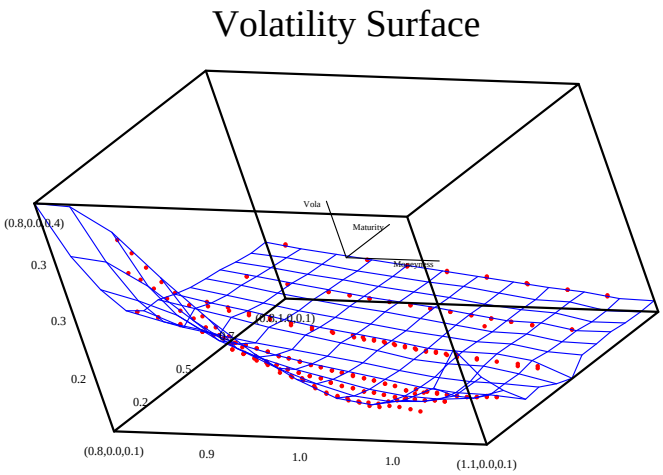

Figure 21: Implied volatility surface with the moneyness and maturity as regressors on January 3, 1997. The red points represent the settlement implied volatilities. The bandwidths are here selected locally.

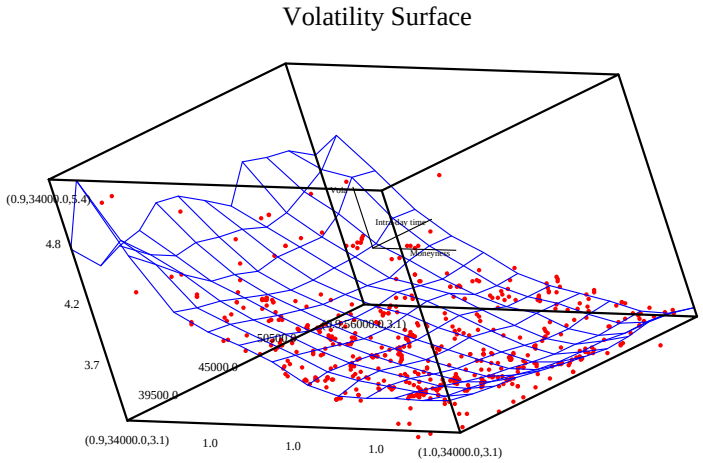

Figure 22: Implied volatility surface with the moneyness and the intra–day time (in seconds) as regressors on January 3, 1997. This surface corresponds to the first series of options, the time to maturity is 14 calendar days. The red points represent the observed option implied volatilities. The EBBS algorithm selects in this case a global bandwidth.

C Nonparametric estimates for different maturities

Figures 23, 24 and 25 does not allow to conclude to an effect of the maturity on the quality of the nonparametric estimates of the implied volatility smile and its derivatives. Particularly, the nonparametric estimates of the second derivative based on local bandwidths still exhibit high unstability. Moreover, the optimal global bandwidth used within the "surface" framework is confirmed as the worst case.

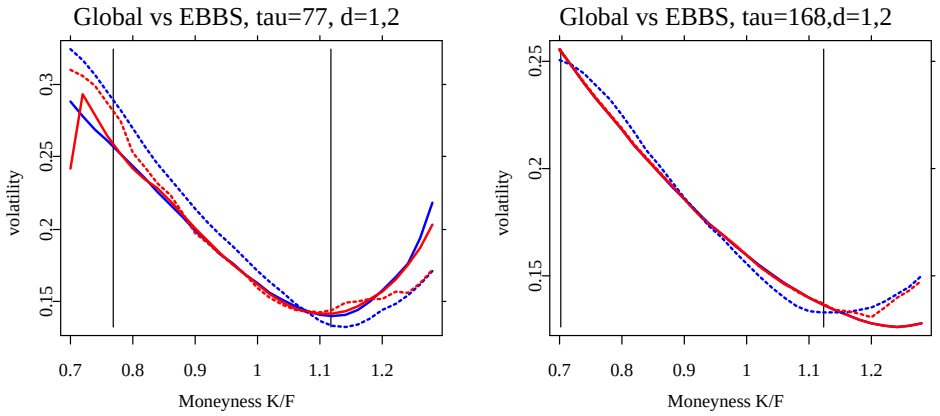

Figure 23: Local polynomial estimates of the volatility smile for both EBBS driven bandwidths (red) and the "optimal" global bandwidth (blue) and using either one (plain) or all maturities (dashed). The left plot correspond to the series whose time to maturity is 77 calendar days and the right to 168 on January 3, 1997.

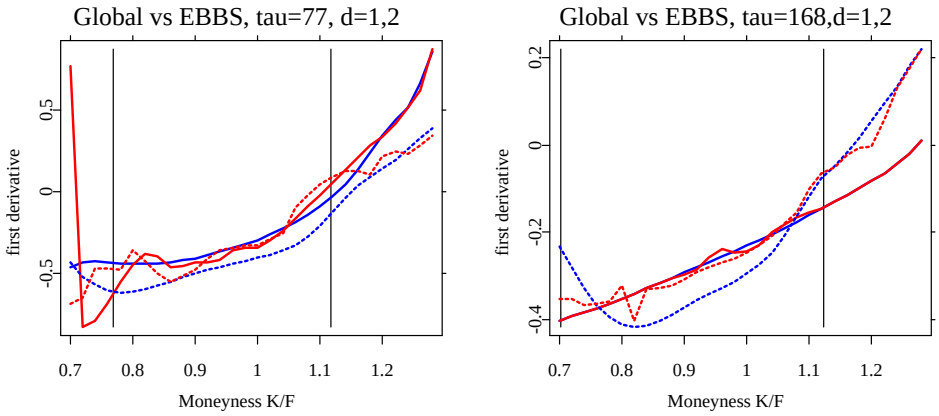

Figure 24: Local polynomial estimates of the first derivative of the volatility smile for both EBBS driven bandwidths (red) and the "optimal" global bandwidth (blue) and using either one (plain) or all maturities (dashed).The left plot correspond to the series whose time to maturity is 77 calendar days and the right to 168 on January 3, 1997.

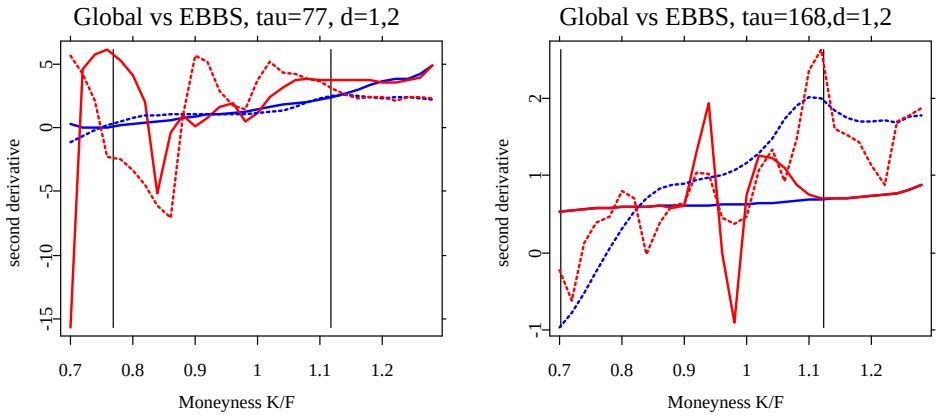

Figure 25: Local polynomial estimates of the second derivative of the volatility smile for both EBBS driven bandwidths (red) and the "optimal" global bandwidth (blue) and using either one (plain) or all maturities (dashed).The left plot correspond to the series whose time to maturity is 77 calendar days and the right to 168 on January 3, 1997.

References

Aït-Sahalia, Y. (1996). The delta method for nonparametric kernel functionals, *Journal of Finance* . mimeo.

Aït-Sahalia, Y. and Duarte, J. (2001). Nonparametric option pricing under shape restrictions. mimeo.

Aït-Sahalia, Y. and Lo, A. W. (1998). Nonparametric estimation of state-price densities implicit in financial asset prices, *Journal of Finance* **53**: 499–547.

Black, F. and Scholes, M. (1973). The pricing of options and corporate liabilities, *Journal of Political Economy* **81**: 637–654.

Breeden, D. and Litzenberger, R. H. (1978). Prices of state-contingent claims implicit in option prices, *Journal of Business* **51**: 621–651.

Derman, E. and Kani, I. (1994). Riding on the Smile, *Risk* **7**: 32–39.

Fan, J. and Gijbels, I. (1996). *Local Polynomial Modelling and Its Application , Vol.66 of Monographs on Statistics and Applied Probability*, Chapman and Hall, New York.

Hafner, R. and Wallmeier, M. (2001). The dynamics of DAX implied volatilities, *Quarterly International Journal of Finance* **1**: 1–27.

Härdle, W. (1990). *Applied Nonparametric Regression*, Cambridge University Press, New York.

Härdle, W., Kleinow, T. and Stahl, G. (2002). *Applied Quantitative Finance*, Springer-Verlag, Berlin.

Hutchinson, J., Lo, A. and Poggio, A. (1994). A nonparametric approach to the pricing and hedging of derivative securities via learning networks, *Journal of Finance* **49**: 851–889.

Manaster and Koehler (1982). The calculation of implied variances from the Black-Scholes model: a note, *Journal of Finance* .

Melick, W. and Thomas, C. (1997). Recovering an asset's implied pdf from option prices: An application to crude oil during the gulf crisis, *Journal of Financial and Quantitative Analysis* **32**: 91–115.

Merton, R. B. (1973). Rational theory of option pricing, *Bell Journal of Economics and Management Science* **4**: 141–183.

Rookley, C. (1997). Fully exploiting the information content of intra-day option quotes: Appliations in option pricing and risk management. mimeo.

Rubinstein, M. (1994). Implied binomial trees, *Journal of Finance* **49**: 771–818.

Ruppert, D. (1997). Empirical-bias bandwidths for local polynomial nonparametric regression and density estimation, *Journal of the American Statistical Association* **92**: 1049–1062.

Ruppert, D. and Wand, M. (1994). Multivariate locally weighted least squares regression, *The Annals of Statistics* **22**: 1346–1370.

Ruppert, D., Wand, M. P., Holst, U. and Hössjer, O. (1997). Local polynomial variance-function estimation, *Technometrics* **39**: 262–273.